5

Copy
RM E53I08

RESEARCH MEMORANDUM

ALTITUDE-CHAMBER INVESTIGATION OF J73-GE-1A TURBOJET ENGINE COMPONENT PERFORMANCE

By Carl E. Campbell and Adam E. Sobolewski

Lewis Flight Propulsion Laboratory
Cleveland, Ohio

NATIONAL ADVISORY COMMITTEE
FOR AERONAUTICS

WASHINGTON

December 9, 1954

NACA RM E53I08

NATIONAL ADVISORY COMMITTEE FOR AERONAUTICS

RESEARCH MEMORANDUM

ALTITUDE-CHAMBER INVESTIGATION OF J73-GE-1A TURBOJET ENGINE COMPONENT PERFORMANCE

By Carl E. Campbell and Adam E. Sobolewski

SUMMARY

An investigation to determine the altitude performance characteristics of a J73-GE-1A turbojet engine was conducted in an altitude chamber at the NACA Lewis laboratory. The engine had a ten-percent oversize turbine-nozzle area compared with the production J73 engine. A fixed-area exhaust nozzle, designed to give limiting temperature at rated speed and static sea-level conditions, was used. Accordingly, the component performance was restricted to those conditions which exist along the engine operating line. The engine was operated over a corrected engine speed range from 83 to 108 percent of rated speed with the variable inlet guide vanes in the open position as normally scheduled for this engine speed range. Data were obtained at simulated altitudes from 15,000 to 55,000 feet and flight Mach numbers from approximately 0.07 to 1.01. The range of Reynolds number index was from 0.90 to 0.20.

A reduction in Reynolds number index from 0.90 to 0.20 lowered the compressor efficiency about 0.025 and the corrected air flow about 2 percent but did not affect the compressor pressure ratio at a given corrected engine speed. At a given corrected turbine speed, there was no noticeable effect of Reynolds number on turbine performance. Total-pressure losses throughout the engine were not affected appreciably by changes in the Reynolds number index. The maximum values of compressor efficiency, turbine efficiency, and combustion efficiency obtained in this investigation were 0.853, 0.865, and 0.96, respectively. The minimum combustion efficiency obtained was about 0.94 at the lowest corrected engine speed (89 percent of rated speed) that was investigated at a Reynolds number index of 0.20. At rated corrected engine speed, the total-pressure loss across the combustor was 0.046 of the combustor-inlet pressure. The compressor-outlet diffuser and the tail-pipe diffuser total-pressure loss ratios were less than 0.01 and 0.03, respectively.

INTRODUCTION

An investigation to determine the altitude-performance characteristics of a J73-GE-1A turbojet engine was conducted in an altitude chamber at the NACA Lewis laboratory. This engine incorporated variable inlet guide vanes as a means of avoiding part-speed surge. The engine also was provided with a 10-percent oversize turbine-nozzle area (compared with the production J73 engine) for the purpose of avoiding stall during flight tests until a more refined automatic control could be developed. The engine incorporated a fixed-area exhaust nozzle designed to give limiting temperature at rated speed and static sea-level conditions. Accordingly, performance of the engine components operating as integral parts of the engine is presented herein only at the conditions that exist along the engine operating line.

3027

Data were obtained over a corrected engine speed range from approximately 83 to 108 percent of rated speed with the variable inlet guide vanes in the open position, as normally scheduled for this engine speed range. The investigation was conducted at simulated altitudes from 15,000 to 55,000 feet with simulated flight Mach numbers from approximately 0.07 to 1.01. The range of Reynolds number index was from approximately 0.90 to 0.20.

Radial pressure and temperature profiles at the engine inlet, compressor outlet, compressor-diffuser outlet, turbine inlet, turbine outlet, and exhaust-nozzle inlet are shown at the extreme ranges of altitude, flight Mach number, and corrected engine speed. Compressor performance and pressure loss data are shown as functions of corrected engine speed, combustion efficiency as a function of combustor-inlet conditions, turbine performance as a function of corrected turbine speed, and exhaust-nozzle performance as a function of exhaust-nozzle pressure ratio. All component performance data are also presented in table I.

INSTALLATION AND INSTRUMENTATION

Engine. - A view of the J73-GE-1A turbojet engine installed in the altitude chamber is shown in figure 1. The engine has variable inlet guide vanes, a 12-stage axial-flow compressor, a cannular-type combustor, a two-stage turbine, and a fixed conical exhaust nozzle with a cold diameter of 20.95 inches. Pending development of a more refined engine control, this engine, along with others of the same model intended for early flight tests, is provided with a turbine-nozzle area ten percent larger than the standard production engines will have in order to avoid compressor surge. Compressor-outlet leakage and bleed air are used as a balance piston force at the front of the compressor and for cooling the turbine disks and the first-stage turbine stator. This air is then

returned to the engine tail pipe downstream of the turbine. At the rated engine speed of 7950 rpm and an exhaust-gas temperature of 1215° F at static sea-level conditions, the rated thrust of the engine is 8630 pounds with an air flow of approximately 142 pounds per second.

Compressor. - The 12-stage axial-flow compressor (fig. 2(a)) has a tip diameter of $32\frac{1}{8}$ inches and a pressure ratio of 6.5:1 at rated engine speed. The hub-tip ratios at the first and twelfth stages are approximately 0.455 and 0.88, respectively. The 21 variable inlet guide vanes rotate simultaneously through an angle of 30° from the open to the closed position. In the open position, the angle between the engine center line and a line tangent to the leading and trailing edges of the guide-vane airfoil sections is zero at the root and 13° at the tip.

Combustor. - The cannular combustion system consists of an annular space containing ten can-type liners that are connected to the turbine-inlet annulus by transition liners (fig. 2(b)). The large elliptical cross-over tubes, which interconnect the ten combustor liners, were designed to facilitate flame propagation during starts at high altitude. A maximum combustor flow area of approximately 5.3 square feet results in an average reference velocity of about 95 feet per second in the combustor.

A fuel nozzle projects into the dome of each of the combustor liners. The fuel nozzles are a duplex design with a large and a small slot supplied by two separate fuel manifolds. Only the small slots function at low fuel flow rates; but as the fuel pressure increases, the flow divider opens and supplies fuel to the large slots as well.

Turbine. - A photograph of the two turbine rotors is shown in figure 2(c). The first-stage turbine rotor contains 57 blades, has a tip diameter of $29\frac{1}{2}$ inches, and has a hub-tip ratio of 0.73. The second-stage turbine rotor has 47 blades, a tip diameter of $31\frac{1}{8}$ inches, and a hub-tip ratio of 0.64. Both rotors have a radial tip clearance of approximately 0.050 inch. The first-stage turbine stator contains 40 vanes which have internal passages for the flow of cooling air obtained from the compressor discharge through the midframe. The second-stage turbine stator has 53 vanes increasing in height from the leading edge to the trailing edge by an amount corresponding to the change in turbine-blade height between the two stages.

Altitude chamber. - The altitude-chamber test section in which the engine was installed is 14 feet in diameter and 20 feet long (fig. 3). The test platform on which the engine was rigidly mounted is connected by a linkage to a balance-pressure diaphragm for measuring engine thrust. A honeycomb is installed in the chamber upstream of the test section to

straighten and smooth the flow of inlet air. The front bulkhead, which incorporates a labyrinth seal around the forward end of the engine, prevents the flow of combustion air directly into the engine compartment and exhaust system, and provides a means of maintaining a pressure difference across the engine. A bellmouth cowl was installed on the front bulkhead just ahead of the engine to obtain a smooth flow of air into the compressor.

Air supplied to the inlet section of the altitude chamber can be either heated or refrigerated dry air, or atmospheric air. Exhaust gases from the jet nozzle pass through an exhaust section, a primary cooler, an exhaust header, and a secondary cooler before entering the exhauster system. The inlet and exhaust pressure controls were designed to maintain automatically a constant ram-pressure ratio and exhaust pressure.

Instrumentation. - The location of instrumentation stations throughout the engine is shown in the cross-sectional sketch of figure 4. Schematic sketches of the instrumentation at the engine inlet, compressor outlet, compressor-diffuser outlet, turbine inlet, turbine outlet, and exhaust-nozzle inlet are shown in figure 5. All pressures were measured by means of alkazene and mercury manometers and were photographically recorded. Temperatures were measured with iron-constantan and chromel-alumel thermocouples and were recorded by self-balancing potentiometers. Engine speed was measured by a chronometric tachometer and fuel flow by means of a calibrated rotameter.

PROCEDURE

Performance characteristics of the engine components were obtained at simulated altitudes from 15,000 to 55,000 feet and flight Mach numbers from 0.07 to 1.01. Engine speed was varied from approximately 6400 rpm to 7950 rpm with the variable inlet guide vanes in the open position. Engine speeds for which the inlet guide vanes are scheduled in the closed position were not investigated because special instrumentation installed on the guide vanes during this portion of the investigation prevented changing their position. Inlet air temperatures from about 44° to -25° F were obtained, but, in general, the standard NACA inlet temperatures were not obtained because of a temporary limitation in the refrigeration system. Therefore, the Reynolds number indices indicated for the various simulated flight conditions differ slightly from those corresponding to standard temperature conditions. The fuel used throughout the investigation was MIL-F-5624A grade JP-4 with a lower heating value of 18,700 Btu per pound and a hydrogen-carbon ratio of 0.168. The symbols and methods of calculation used to determine the performance of components along an engine operating line are given in appendixes A and B.

RESULTS AND DISCUSSION

Radial Pressure and Temperature Profiles

In order to define the environmental conditions under which each of the engine components operates at various flight conditions and engine speeds, radial pressure and temperature profiles measured at several stations within the engine are presented in figures 6 to 11. These data not only indicate the inlet conditions for a given component but also show the effect of each component in changing the radial profile of pressure and temperature of the gas in passing through that component. Profiles are presented in the form of an average radial pressure or temperature divided by the over-all average pressure or temperature in order to compare profiles at different pressure and temperature levels. The average radial pressure or temperature is an average of from two to four circumferential measurements at the same radial location.

As would be expected, both the temperature profile and the total- and static-pressure profiles at the engine inlet were extremely flat with the exception of a slight reduction of total pressure near the outside wall due to boundary-layer build-up (fig. 6). This boundary layer existed in the outer 10 percent of the passage height, and the maximum total-pressure deficit measured was about 1 percent of the average pressure.

At the compressor outlet (fig. 7), the total pressure was found to vary by as much as $\pm 2\frac{1}{2}$ percent of the average total pressure, with the lowest value occurring near the blade root (inner wall) at all operating conditions. Coupled with the higher temperature at the root (fig. 7(b)), it appears that the root-section efficiency is appreciably lower than the average compressor efficiency, particularly at high engine speeds. The temperature measurements, however, are too meager to accurately define the radial efficiency distribution. As the corrected engine speed was reduced from approximately rated speed, the peak pressure moved inward from 50 percent of the passage height to 27 percent, the pressure at the blade root increased, and the pressure at the tip decreased. Inasmuch as the temperature near the root was lowered with engine speed, the root-section efficiency was apparently improved as the speed decreased. The inflection point shown by most of the total-pressure curves at 72 percent passage height may be due to the wake from an annular splitter vane which was located just upstream of the instrumentation at a passage height of 65 percent. The function of the splitter vane is to prevent flow separation from the inner walls of the diffuser conducting the flow from the compressor outlet into the combustor section.

Profiles of total pressure obtained from a single rake near the outlet of the diffuser are shown in figure 8. At low engine speeds, the

profiles were similar to those at the compressor outlet. However, at high engine speeds the peak pressure shifted toward the outer wall, indicating that the flow tends to break away somewhat from the sloping diffuser inner wall at high engine speeds.

At the turbine inlet (fig. 9), there was no discernible effect of engine speed or flight condition on the total-pressure profiles. The same general profile shape existed at the turbine inlet as at the compressor outlet in that peak pressure occurred near midpassage and the pressure at the inner wall was lower than at the outer wall. However, the maximum deviation from the average turbine-inlet total pressure did not exceed ±1/2 of 1 percent.

Radial profiles of total pressure and temperature at the turbine outlet (station 6) are shown in figure 10. The total pressure reached peak values between 20 and 40 percent of the passage height from the blade root and dropped off toward either wall. There were no significant effects of engine speed or flight conditions on the profile. The total-temperature profiles were similar for all conditions shown except for operation at a corrected engine speed of 7996 rpm, an altitude of 15,000 feet, and a flight Mach number of 0.8. At this condition, the peak temperature shifted radially inward from the average position at 50 percent of the passage height to 26 percent of the passage height. Such a trend might be serious inasmuch as the maximum permissible gas temperature is lower near the turbine blade roots than near the blade tips as a result of the higher root stresses. Data were not obtained at lower altitudes and therefore this apparent trend cannot be verified.

Similar profiles obtained at station 7 in the exhaust nozzle are presented in figure 11. Both the pressure and temperature profiles are quite similar to those at the turbine outlet over comparable ranges of percent of passage height. A comparison of the pressure profile does, however, indicate an appreciable pressure loss near the outer wall of the tail-pipe assembly.

In order to summarize the trends indicated by the pressure and temperature profiles, it can be stated that the total-pressure profiles at various stations throughout the engine were, in general, unaffected by changes in Reynolds number index. At high engine speeds, the total-pressure profile shifted toward the outer wall at the compressor-diffuser outlet, but this effect disappeared at the turbine inlet. The temperature profiles showed no appreciable effects of Reynolds number index or engine speed with the exception of a turbine-outlet peak temperature shift toward the root at the highest pressure level investigated.

Compressor Performance

The corrected compressor air flow obtained at each Reynolds number index is shown in figure 12(a) over the range of corrected engine

speeds investigated. At a Reynolds number index of 0.90 and rated corrected engine speed of 7950 rpm, the corrected compressor air flow was 142 pounds per second. Reducing the Reynolds number index to 0.20 at the same corrected speed lowered the corrected air flow to 139.5 pounds per second. The relatively steep slope of the air-flow curves at rated speed indicates that the engine can operate at appreciably higher corrected speeds before the air flow becomes choked at the compressor inlet.

The effects of corrected engine speed and Reynolds number index on compressor efficiency are shown in figure 12(b). Peak values of compressor efficiency occurred at corrected engine speeds between 85 and 90 percent of rated speed for all Reynolds number indices and were about 3 percent higher than the efficiency values obtained at rated speed. The maximum compressor efficiency obtained in this investigation was 0.853 at a Reynolds number index of 0.90 and a corrected engine speed of about 7100 rpm. At a given corrected engine speed, lowering the Reynolds number index from 0.90 to 0.20 reduced the compressor efficiency about 0.025.

Compressor total-pressure ratio is presented in figure 12(c) as a function of corrected engine speed for the range of Reynolds number indices investigated. The compressor pressure ratio generalized with corrected engine speed for all values of Reynolds number index. In most axial-flow turbojet engines, the pressure ratio increases slightly with lower Reynolds number indices (see ref. 1); however, the effects of decreased corrected air flow and compressor efficiency combined with the attendant increase in corrected turbine-inlet temperature as the Reynolds number index was lowered were such that the compressor operating line did not shift in this engine. Therefore, the reductions in corrected air flow and compressor efficiency discussed previously are due to Reynolds number effects alone (figs. 12(a) and (b)). Compressor pressure ratio increased almost linearly with increased corrected engine speed up to about rated speed and increased at a slightly lower rate thereafter. At corrected engine speeds of 7950 rpm (rated speed) and 8600 rpm (maximum speed obtained), the values of compressor pressure ratio were 6.5 and 7.3, respectively.

The compressor-outlet-diffuser total-pressure losses were less than 1 percent of the diffuser-inlet total pressure as shown in figure 13. The total-pressure loss ratio reached a peak at a corrected engine speed of 7600 rpm and was not noticeably affected by changes in Reynolds number index.

Combustor Performance

Combustion efficiencies obtained at all flight conditions and engine speeds are shown in figure 14(a) as a function of the combustor-inlet parameter P_4T_4/V_R, which is derived in reference 2. Over the

range of flight conditions and engine speeds investigated, combustor-inlet pressure varied from 1830 to 11,800 pounds per square foot, combustor-inlet temperature varied from 769° to 927° R, and the average combustor reference velocity was about 95 feet per second. For this range of combustor-inlet conditions, combustion efficiencies ranged from 0.94 to 0.96. The trend of the data at the lowest values of P_4T_4/V_R indicates that the combustion efficiency would start to decrease rapidly at a Reynolds number index of 0.20 if the corrected engine speed were lowered appreciably beyond the minimum value of 7059 rpm obtained in this investigation. However, in the range of normal operating speeds at Reynolds number indices of 0.24 and 0.20, which correspond to transonic flight Mach numbers at altitudes of 49,000 and 55,000 feet, respectively, the combustion efficiency was 0.94 or higher.

The combustor total-pressure loss ratio (fig. 14(b)) decreased from about 0.055 at the lowest corrected engine speed investigated to an average value for all flight conditions of about 0.046 at a corrected engine speed of 7950 rpm. In general, the total-pressure loss ratio increased very slightly as Reynolds number index was reduced. This increase was due to the increased momentum pressure loss resulting from the higher combustor temperature rise required at the lower Reynolds number indices as compressor efficiency became lower.

Turbine Performance

The variation of turbine efficiency, turbine pressure ratio, and corrected turbine gas flow with corrected turbine speed is shown in figure 15. Turbine efficiency increased from about 0.815 at the lowest corrected turbine speed of 3855 rpm to a peak of 0.865 at a corrected turbine speed of about 4075 rpm. This variation of turbine efficiency is almost entirely an effect of corrected turbine speed inasmuch as the turbine pressure ratio was essentially constant at 2.7 for all flight conditions and engine conditions investigated. Within the accuracy of the data, there was no discernible turbine Reynolds number effect on turbine efficiency. All turbine efficiencies obtained at a Reynolds number index of 0.90 were in the neighborhood of 0.86. As the Reynolds number index was reduced, the increased turbine-inlet temperature required as compressor efficiency dropped off resulted in a shift to lower corrected turbine speeds for a given corrected engine speed, or a shift away from the region of peak turbine efficiency. At a Reynolds number index of 0.20, the turbine efficiency was still about 0.86 at a corrected engine speed of 8093 rpm but decreased to 0.84 at a corrected engine speed of 7059 rpm.

As shown in figure 15, the variation of corrected turbine gas flow with corrected turbine speed generalized for all flight conditions investigated; it was impossible to determine a turbine Reynolds number

effect on corrected turbine gas flow because of the limited amount and accuracy of the data. The constant value of corrected turbine gas flow with the variations of corrected turbine speed indicates that the first-stage turbine nozzles were choked at all flight conditions and engine conditions investigated. Calculations based on the choked corrected gas flow value of 47.2 pounds per second show the effective turbine-nozzle area to be about 0.95 square foot.

3027

Tail-Pipe-Diffuser and Exhaust-Nozzle Performance

The tail-pipe-diffuser total-pressure loss was less than 3 percent of the turbine-outlet total pressure as shown in figure 16. The total-pressure loss ratio reached a peak value at a corrected engine speed of approximately 7600 rpm and did not show a variation with Reynolds number index.

CH-2

The exhaust-nozzle flow coefficient and thrust coefficient are shown in figure 17 as functions of exhaust-nozzle pressure ratio (ratio of nozzle-inlet total pressure to free-stream static pressure). The nozzle flow coefficient is defined as the ratio of effective nozzle area to geometric area and can be expressed as the ratio of mass flow determined at the engine inlet to the mass flow calculated by using the nozzle-inlet measurements and the exhaust-nozzle-outlet area. At exhaust-nozzle pressure ratios above approximately 2.2, the flow coefficient was constant at a value of 0.99. Decreasing the nozzle pressure ratio to 1.6 lowered the flow coefficient to 0.97.

The exhaust-nozzle thrust coefficient, which is a measure of the ratio of actual jet velocity to ideal jet velocity downstream of the nozzle exit, was determined from the ratio of scale jet thrust to rake jet thrust. At all values of exhaust-nozzle pressure ratio investigated, the thrust coefficient was constant at a value of about 1.00. The values of thrust coefficient or velocity coefficient obtained in this investigation are approximately 2 percent higher than would be expected according to other investigations (see ref. 3) of similar exhaust nozzles (outlet diameter, 20.95 in.; cone half-angle, 6°). These high values of thrust coefficient are attributed primarily to errors in the average total pressure at the exhaust-nozzle inlet because of the fact that a large total-pressure gradient existed at that station (see fig. 11(a)). For this reason also, the values of the flow coefficient may be slightly higher than the true values.

SUMMARY OF RESULTS

From an altitude-chamber investigation of the component performance of a J73-GE-1A turbojet engine, the following results were obtained:

1. Pressure and temperature profiles throughout the engine showed no significant effects of flight condition or engine speed with the possible exception of a slight shift in maximum turbine-outlet temperature toward the root at the highest pressure level investigated.

2. The maximum compressor efficiency obtained was 0.853 at a Reynolds number index of 0.90 and a corrected engine speed of about 7100 rpm. A reduction in Reynolds number index from 0.90 to 0.20 lowered the compressor efficiency about 0.025 and lowered the corrected air flow about 2 percent, on the average, but did not affect the compressor pressure ratio at a given corrected engine speed.

3. The combustion efficiency was 0.94 or higher in the range of normal operating speeds at Reynolds number indices of 0.24 and 0.20, which correspond to transonic flight Mach numbers at altitudes of 49,000 and 55,000 feet, respectively. The total-pressure loss ratio across the combustor was about 0.046 at a corrected engine speed of 7950 rpm (rated speed).

4. Over the range of engine speeds investigated, turbine efficiency was approximately 0.86 at a Reynolds number index of 0.90. At a Reynolds number index of 0.20, turbine efficiency varied from 0.86 at a corrected engine speed of 8093 rpm to 0.84 at a corrected engine speed of 7059 rpm. At a given corrected turbine speed, there was no discernible effect of Reynolds number on turbine performance.

5. At exhaust-nozzle pressure ratios above 2.2, the exhaust-nozzle flow coefficient was constant at a value of 0.99. The exhaust-nozzle thrust coefficient was constant at a value of 1.00 at all values of exhaust-nozzle pressure ratio. These values of flow coefficient and thrust coefficient are believed to be somewhat higher than their true value primarily because of errors in the average total pressure at the exhaust-nozzle inlet. The compressor-outlet-diffuser and tail-pipe-diffuser total-pressure loss ratios reached peak values at a corrected engine speed of 7600 rpm and were less than 0.01 and 0.03, respectively.

Lewis Flight Propulsion Laboratory
National Advisory Committee for Aeronautics
Cleveland, Ohio, September 4, 1953

APPENDIX A

SYMBOLS

The following symbols are used in this report:

A	area, sq ft
B	test-bed balance force, lb
C_D	exhaust-nozzle flow coefficient
C_T	exhaust-nozzle thrust coefficient
F_j	jet thrust, lb
f	fuel-air ratio
g	acceleration due to gravity, 32.2 ft/sec^2
h	enthalpy of air or gas mixture, Btu/lb
M	Mach number
N	engine speed, rpm
P	total pressure, lb/sq ft abs
p	static pressure, lb/sq ft abs
R	gas constant, 53.4 ft-lb/lb-$^\circ$R
T	total temperature, $^\circ$R
T_i	indicated temperature, $^\circ$R
V	velocity, ft/sec
V_R	combustor reference velocity, ft/sec
W_a	air flow, lb/sec
W_f	fuel consumption, lb/hr
W_g	gas flow, lb/sec
α	thermocouple impact recovery factor, 0.85

γ ratio of specific heats

δ pressure correction factor, P/2116 (total pressure divided by NACA standard sea-level pressure)

η efficiency

θ temperature correction factor, $\gamma T/(1.4)(519)$, (product of γ and total temperature divided by product of γ and temperature for air at NACA standard sea-level conditions)

λ $\frac{Am + B}{m + 1}$ (see ref. 5), Btu/lb of fuel

ρ density, slugs/cu ft

φ ratio of absolute viscosity of air at engine inlet to absolute viscosity of NACA standard atmosphere at sea level

$\delta/\varphi\sqrt{\theta}$ Reynolds number index

Subscripts:

a air

act actual

b combustor

c compressor

eff effective

g gas mixture

isen isentropic

n exhaust-nozzle outlet

r rake

s scale

t turbine

x engine-inlet duct

0 free stream

1	engine inlet
3	compressor outlet
4	combustor inlet
5	turbine inlet
6	turbine outlet (tail-pipe diffuser inlet)
7	exhaust-nozzle inlet (tail-pipe diffuser outlet)

[redacted]

APPENDIX B

METHODS OF CALCULATION

Total temperatures were calculated from thermocouple indicated temperatures with the equation

$$T = \frac{T_i\left(\frac{P}{p}\right)^{\frac{\gamma-1}{\gamma}}}{1 + \alpha\left[\left(\frac{P}{p}\right)^{\frac{\gamma-1}{\gamma}} - 1\right]} \tag{1}$$

Air flow. - Engine-inlet air flow was determined from pressure and temperature instrumentation at station 1 by use of the equation

$$W_{a,1} = g\rho_1 A_1 V_1 = p_1 A_1 \sqrt{\frac{2\gamma_1}{\gamma_1 - 1}\frac{g}{RT_1}\left(\frac{P_1}{p_1}\right)^{\frac{\gamma_1-1}{\gamma_1}}\left[\left(\frac{P_1}{p_1}\right)^{\frac{\gamma_1-1}{\gamma_1}} - 1\right]} \tag{2}$$

The various compressor-outlet bleed flows and compressor leakage air were determined to be about 2 percent of the inlet air flow. All bleed and leakage flows rejoined the main-stream mass flow before passing through the exhaust nozzle.

Compressor efficiency. - Compressor efficiency was calculated by using the air tables of reference 4 and by neglecting the water-vapor corrections. With the compressor pressure ratio and the compressor inlet and outlet temperatures known, the compressor efficiency was determined from the following expression:

$$\eta_c = \frac{\Delta h_{isen}}{\Delta h_{act}} = \frac{h_{3,isen} - h_1}{h_{3,act} - h_1} \tag{3}$$

Turbine-inlet temperature. - Turbine-inlet temperature was determined from enthalpy-temperature tables after the enthalpy of the gas at the turbine inlet was calculated as follows:

$$h_{g,5} = \frac{W_{a,1}(h_{a,3} - h_{a,1})}{0.98W_{a,1} + \frac{W_f}{3600}} + h_{g,7} \tag{4}$$

Combustion efficiency. - Combustion efficiency is defined as the ratio of the actual enthalpy rise through the combustor to the theoretical maximum enthalpy rise. The following equation was used to calculate combustion efficiency:

$$\eta_b = \frac{h_{a,7} + f\lambda_7 - h_{a,1}}{18{,}700f} \tag{5}$$

where 18,700 Btu per pound of fuel is the lower heating value of the fuel and f is the ratio of fuel flow to engine-inlet air flow.

Turbine efficiency. - The turbine adiabatic efficiency was determined from the following equation:

$$\eta_t = \frac{1 - \frac{T_7}{T_5}}{\frac{\frac{\gamma_t - 1}{\gamma_t}}{1 - \left(\frac{P_6}{P_5}\right)}} \tag{6}$$

where γ_t is the average value of γ between stations 5 and 7.

Exhaust-nozzle flow coefficient. - The flow coefficient was calculated as the ratio of mass flow determined at the engine inlet (eq. (2)) to the mass flow calculated at the exhaust-nozzle outlet. The exhaust-nozzle-outlet mass flow was calculated as follows:

$$W_{g,n} = p_n A_n \sqrt{\frac{2\gamma_7}{(\gamma_7 - 1)} \frac{g}{RT_7} \left(\frac{P_7}{p_n}\right)^{\frac{\gamma_7 - 1}{\gamma_7}} \left[\left(\frac{P_7}{p_n}\right)^{\frac{\gamma_7 - 1}{\gamma_7}} - 1\right]} \tag{7}$$

When the nozzle was choked, p_n was calculated from the pressure ratio required for choking as determined by γ_7. When the nozzle was not choked, p_n was assumed equal to p_0.

Exhaust-nozzle thrust coefficient. - The thrust coefficient was calculated as the ratio of scale jet thrust to rake jet thrust. Scale thrust was obtained from the equation

$$F_{j,s} = B + \frac{W_{a,1}V_x}{g} + A_x(p_x - p_0) \tag{8}$$

The rake jet thrust was calculated from the mass flow determined at the engine inlet and from an effective velocity determined by the exhaust-gas total temperature, the ratio of specific heats, and the exhaust-nozzle pressure ratio. The expression used, which represents the thrust of a convergent nozzle, was

$$F_{j,r} = \frac{(W_{a,1} + W_f/3600)}{g} V_{eff} \tag{9}$$

3027

The effective velocity parameter includes the excess of pressure beyond that converted to velocity for supercritical pressure ratios (see ref. 6).

REFERENCES

1. Prince, William R., and Jansen, Emmert T.: Altitude-Wind-Tunnel Investigation of Compressor Performance on J47 Turbojet Engine. NACA RM E9G28, 1949.

2. Childs, J. Howard: Preliminary Correlation of Efficiency of Aircraft Gas-Turbine Combustors for Different Operating Conditions. NACA RM E50F15, 1950.

3. Wallner, Lewis E., and Wintler, John T.: Experimental Investigation of Typical Constant- and Variable-Area Exhaust Nozzles and Effects on Axial-Flow Turbojet-Engine Performance. NACA RM E51D19, 1951.

4. Amorosi, A.: Gas Turbine Gas Charts. Res. Memo. No. 6-44 (Navships 250-330-6), Bur. Ships, Navy Dept., Dec. 1944.

5. Turner, L. Richard, and Bogart, Donald: Constant-Pressure Combustion Charts Including Effects of Diluent Addition. NACA Rep. 937, 1949. (Supersedes NACA TN's 1086 and 1655.)

6. Turner, L. Richard, Addie, Albert N., and Zimmerman, Richard H.: Charts for the Analysis of One-Dimensional Steady Compressible Flow. NACA TN 1419, 1948.

[redacted]

TABLE I. - COMPONENT PERFORMANCE DATA FOR J75-GE-1A TURBOJET ENGINE

Run	Altitude, ft	Reynolds number index, $\frac{\delta_1}{\theta_1\sqrt{\theta_1}}$	Ram-pressure ratio, P_1/P_0	Flight Mach number, M_0	Tank static pressure, p_0, lb/sq ft abs	Engine speed, N, rpm	Fuel flow, W_f, lb/hr	Engine-inlet total pressure, P_1, lb/sq ft abs	Engine-inlet total temperature, T_1, °R	Compressor-outlet total pressure, P_3, lb/sq ft abs	Compressor-outlet total temperature, T_3, °R	Combustor-inlet total pressure, P_4, lb/sq ft abs	Turbine-inlet total pressure, P_5, lb/sq ft abs	Turbine-inlet total temperature, T_5, °R	Turbine-outlet total pressure, P_6, lb/sq ft abs	Exhaust-nozzle-inlet total pressure, P_7, lb/sq ft abs
1	15,000	0.896	1.526	0.803	1185	7841	7500	1811	498	11,858	927	11,768	11,235	2033	4191	4087
2		.893	1.511	.792	1194	7737	7120	1804	499	11,680	919	11,573	11,042	1980	4115	4003
3		.899	1.520	.798	1191	7814	6680	1810	498	11,330	906	11,247	10,728	1920	3996	3885
4		.898	1.513	.795	1193	7216	5380	1808	498	10,192	870	10,118	9,648	1747	3582	3484
5		.910	1.533	.806	1192	6581	3370	1827	496	8,219	811	8,193	7,741	1460	2840	2787
6	15,000	0.749	1.269	0.594	1193	7822	6160	1514	499	9,855	926	9,790	9,357	2023	3509	3396
7		.749	1.277	.602	1179	7778	6125	1506	497	9,852	921	9,788	9,340	1998	3490	3393
8		.761	1.284	.609	1184	7815	5670	1520	495	9,519	906	9,450	9,023	1933	3364	3272
9		.750	1.279	.604	1181	7222	4530	1511	497	8,525	872	8,467	8,072	1756	2999	2916
10		.759	1.272	.597	1191	6680	3120	1515	496	7,119	820	7,096	6,721	1510	2473	2426
11	15,000	0.651	1.102	0.376	1197	7828	5450	1319	499	8,603	926	8,539	8,153	2030	3048	2966
12		.661	1.112	.392	1187	7212	3958	1320	495	7,477	868	7,417	7,082	1780	2629	2557
13		.668	1.118	.403	1187	6411	2545	1327	493	5,855	796	5,835	5,528	1447	2019	1980
14	15,000	0.594	1.006	0.092	1183	7795	4855	1190	494	7,715	922	7,661	7,319	2018	2729	2657
15		.588	.994	-----	1188	7598	4370	1182	488	7,580	904	7,526	6,996	1957	2609	2539
16		.601	1.002	.055	1187	7222	3800	1188	492	6,738	871	6,684	6,376	1780	2391	2324
17		.596	1.010	.118	1178	6407	2250	1180	493	5,157	799	5,142	4,863	1497	1888	1852
18	25,000	0.580	1.526	0.802	781	7839	4800	1192	495	7,794	924	7,737	7,396	2029	2759	2682
19		.593	1.524	.800	780	7786	4770	1189	493	7,729	918	7,674	7,331	2000	2736	2658
20		.585	1.537	.809	778	7827	4255	1198	494	7,423	904	7,379	7,034	1940	2636	2561
21		.589	1.529	.803	777	6551	2175	1188	495	5,303	805	5,281	4,991	1455	1843	1797
22	35,000	0.550	1.912	1.009	486	7875	4480	929	435	6,778	863	6,729	6,428	2013	2388	2336
23		.551	1.898	1.003	490	7817	3930	930	436	6,455	840	6,409	6,123	1890	2268	2217
24		.541	1.912	1.009	489	7214	3240	938	440	5,888	806	5,861	5,581	1728	2074	2018
25		.531	1.912	1.009	491	6678	2500	939	449	4,941	768	4,921	4,678	1503	1728	1688
26	35,000	0.412	1.548	0.816	495	7848	3340	787	468	5,165	900	5,132	4,905	2040	1827	1780
27		.410	1.527	.802	490	7807	3290	748	461	5,181	884	5,183	4,915	2007	1812	1775
28		.377	1.538	.809	489	7797	3090	752	491	4,889	921	4,862	4,642	2033	1732	1684
29		.373	1.548	.816	487	7817	2800	754	497	4,857	911	4,837	4,430	1957	1651	1601
30		.408	1.538	.809	489	7816	3010	782	485	4,949	874	4,922	4,694	1890	1739	1689
31		.402	1.532	.806	491	7438	2770	752	471	4,797	865	4,763	4,545	1863	1689	1841
32		.401	1.546	.816	494	7214	2400	749	474	4,429	847	4,389	4,204	1767	1555	1518
33		.387	1.544	.813	493	7174	2205	761	504	4,175	878	4,160	3,956	1763	1488	1422
34		.388	1.546	.815	485	6678	1666	750	482	3,649	807	3,640	3,482	1537	1273	1238
35	45,000	0.247	1.787	0.950	254	7699	1830	454	468	3,061	891	3,038	2,898	1988	1080	1045
36		.242	1.764	.934	260	7625	1880	456	470	3,024	886	3,018	2,871	1954	1051	1035
37		.238	1.796	.955	251	7220	1500	449	475	2,684	858	2,667	2,547	1803	925	910
38		.250	1.761	.937	259	6984	1340	456	486	2,581	821	2,552	2,427	1690	869	876
39		.229	1.739	.928	257	6880	1050	447	486	2,190	818	2,189	2,069	1570	756	742
40	55,000	0.191	1.961	1.031	179	7661	1830	351	465	2,352	888	2,346	2,236	2000	820	808
41		.195	1.816	.985	197	7508	1441	358	461	2,315	868	2,305	2,194	1850	807	794
42		.188	1.940	1.022	185	7225	1270	355	464	2,178	848	2,168	2,063	1817	751	741
43		.193	1.875	.992	189	6988	1078	354	465	1,995	821	1,991	1,892	1700	692	683
44		.205	1.994	1.045	181	6674	892	361	464	1,830	784	1,830	1,736	1580	633	624

TABLE I. - Concluded. COMPONENT PERFORMANCE DATA FOR J73-GE-1A TURBOJET ENGINE

Run	Exhaust-gas total temperature, T_7, °R	Engine-inlet air flow, $W_{a,1}$, lb/sec	Corrected engine-inlet air flow, $\frac{W_{a,1}\sqrt{\theta_1}}{\delta_1}$, lb/sec	Corrected engine speed, $\frac{N}{\sqrt{\theta_1}}$, rpm	Compressor total-pressure ratio, P_3/P_1	Compressor efficiency, η_c	Fuel-air ratio, $\frac{W_f}{3600W_{a,1}}$	Combustor total-pressure loss ratio, $\frac{(P_4 - P_5)}{P_4}$	Combustion efficiency, η_b	Corrected turbine speed, $\frac{N}{\sqrt{\theta_5}}$, rpm	Corrected turbine gas flow, $\frac{W_{g,5}\sqrt{\theta_5}}{\delta_5\left(\frac{\gamma_5}{1.4}\right)}$, lb/sec	Turbine total-pressure ratio, P_5/P_8	Turbine efficiency, η_t	Exhaust-nozzle pressure ratio, P_7/P_0	Exhaust-nozzle flow coefficient, C_D	Exhaust-nozzle thrust coefficient, C_T
1	1664	124.3	142.3	7998	6.548	0.820	0.0188	0.0453	0.961	4092	47.65	2.581	0.854	3.449	0.996	0.997
2	1614	123.0	141.4	7890	6.483	.829	.0181	.0469	.954	4087	47.27	2.885	.866	3.353	.989	.998
3	1554	121.7	139.3	7775	6.280	.834	.0153	.0452	.956	4078	47.33	2.886	.860	3.262	.991	.998
4	1411	114.7	131.7	7567	5.647	.851	.0130	.0485	.949	4040	47.08	2.893	.874	2.920	.985	.985
5	1176	101.7	115.3	6719	4.499	.849	.0092	.0552	.976	4003	47.05	2.726	.848	2.338	.988	.976
6	1650	103.8	142.4	7977	6.509	0.820	0.0185	0.0483	0.965	4091	47.79	2.861	0.873	2.847	0.988	1.004
7	1628	103.3	142.1	7948	6.542	.823	.0165	.0456	.945	4092	47.24	2.676	.872	2.878	.987	.997
8	1570	102.8	139.8	7798	6.263	.823	.0153	.0452	.954	4086	47.75	2.682	.876	2.784	.997	.994
9	1422	96.01	131.5	7380	5.642	.841	.0131	.0467	.954	4038	47.22	2.692	.884	2.489	.994	.996
10	1220	86.91	118.7	6833	4.699	.847	.0100	.0827	.963	4002	47.21	2.717	.843	2.037	.991	.987
11	1639	90.21	141.8	7983	6.522	0.822	0.0168	0.0452	0.955	4088	47.65	2.675	0.882	2.478	0.995	1.008
12	1428	83.97	131.4	7385	5.884	.846	.0131	.0451	.963	4025	47.14	2.694	.857	2.154	.990	.998
13	1172	70.52	109.6	6578	4.281	.850	.0092	.0545	.977	3919	47.18	2.639	.848	1.686	.974	1.010
14	1644	81.48	141.3	7990	6.482	0.808	0.0166	0.0448	0.959	4083	47.81	2.682	0.872	2.246	0.997	1.005
15	1578	78.00	138.3	7772	6.244	.829	.0154	.0450	.965	4054	47.35	2.682	.862	2.135	.990	1.008
16	1440	75.32	130.5	7417	5.667	.827	.0133	.0481	.966	4008	47.23	2.667	.861	1.958	.981	1.018
17	1221	83.36	109.8	6574	4.334	.835	.0098	.0543	.965	3855	47.36	2.579	.806	1.572	.971	1.019
18	1654	81.48	141.2	8027	6.539	0.811	0.0167	0.0441	0.960	4093	47.44	2.681	0.858	3.434	0.992	0.993
19	1633	81.15	140.8	7989	6.500	.812	.0163	.0447	.986	4084	47.24	2.680	.858	3.408	.990	.994
20	1576	80.08	138.2	7818	6.207	.817	.0147	.0487	1.009	4086	47.75	2.668	.877	3.292	.993	.998
21	1176	65.88	114.8	6708	4.464	.847	.0092	.0549	.980	3995	47.19	2.708	.838	2.315	.994	.971
22	1642	70.04	148.1	8602	7.294	0.773	0.0178	0.0447	0.934	4130	46.76	2.692	0.864	4.807	0.976	0.994
23	1540	69.18	144.2	8311	6.939	.795	.0158	.0446	.961	4115	46.80	2.700	.855	4.524	.980	.987
24	1399	66.55	138.7	7834	6.297	.829	.0135	.0462	.955	4067	46.80	2.691	.858	4.127	.983	.984
25	1217	60.04	125.8	7180	5.262	.849	.0106	.0494	.959	4011	46.80	2.707	.839	3.438	.983	.977
26	1665	55.99	141.5	8265	6.731	0.778	0.0172	0.0442	0.963	4090	47.57	2.685	0.865	3.596	0.993	1.017
27	1639	53.66	143.1	8283	6.926	.799	.0170	.0480	.953	4098	46.74	2.712	.852	3.822	.983	1.000
28	1661	50.94	139.4	8016	6.501	.800	.0168	.0452	.958	4087	47.30	2.680	.864	3.444	.990	1.007
29	1585	49.87	136.9	7784	6.190	.812	.0156	.0446	.967	4047	47.48	2.685	.864	3.287	.998	1.007
30	1569	53.20	141.7	8048	6.581	.805	.0157	.0465	.981	4081	47.33	2.688	.846	3.474	.993	1.008
31	1517	52.02	139.5	7808	6.379	.828	.0148	.0458	.984	4041	46.98	2.691	.856	3.342	.987	1.004
32	1434	49.81	133.9	7548	5.915	.835	.0134	.0443	.986	4017	47.05	2.703	.855	3.132	.988	1.020
33	1431	46.77	128.1	7280	5.486	.838	.0131	.0470	.988	3999	47.08	2.698	.856	2.884	.991	.982
34	1242	44.10	118.8	6927	4.865	.842	.0105	.0517	.982	3969	47.14	2.711	.847	2.553	.994	1.002
35	1619	32.18	142.5	8108	6.720	0.794	0.0167	0.0468	0.951	4059	47.28	2.732	0.855	4.114	0.994	1.000
36	1594	31.78	140.2	8011	6.652	.804	.0164	.0481	.939	4053	48.66	2.731	.848	3.981	.981	1.012
37	1460	29.19	131.6	7547	5.978	.826	.0143	.0480	.935	3985	48.17	2.753	.851	3.625	.979	1.006
38	1364	29.25	128.6	7349	5.616	.832	.0127	.0490	.952	3961	46.88	2.730	.861	3.382	.980	1.000
39	1289	25.94	118.8	6903	4.899	.836	.0112	.0548	.941	3932	48.78	2.737	.842	2.887	.988	.958
40	1630	25.41	145.0	8093	6.701	0.788	0.0167	0.0469	0.964	4028	48.56	2.727	0.856	4.514	1.019	0.977
41	1572	24.89	139.4	7965	6.503	.795	.0161	.0481	.947	4015	47.52	2.719	.852	4.030	.997	.987
42	1476	23.91	134.8	7839	6.135	.820	.0148	.0478	.929	3973	48.98	2.747	.844	4.049	.992	.983
43	1381	23.01	129.9	7367	5.836	.822	.0130	.0497	.950	3947	47.48	2.734	.837	3.614	.998	.985
44	1278	21.76	120.8	7059	5.069	.828	.0114	.0514	.955	3917	47.05	2.743	.840	3.448	.989	.989

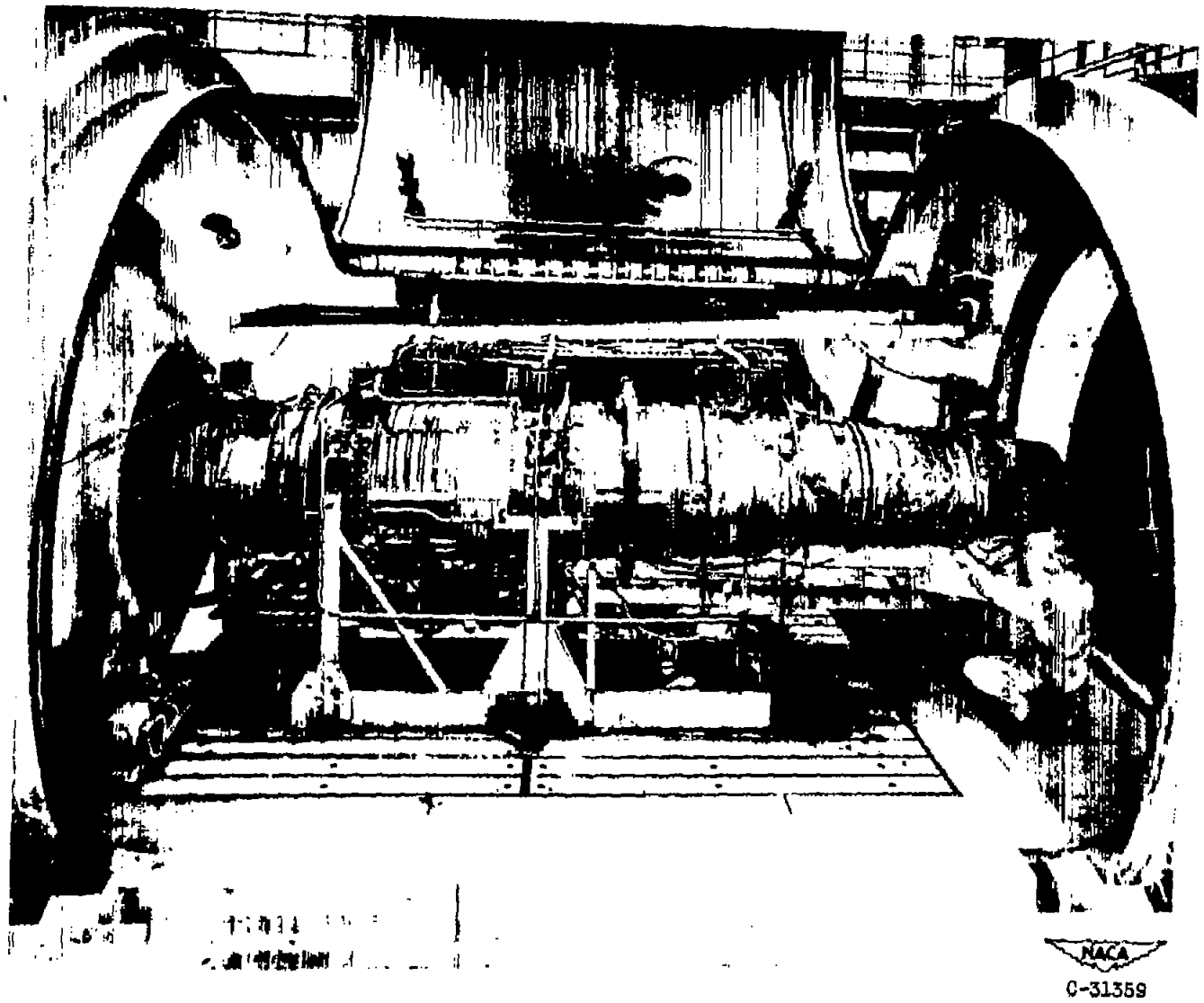

C-31359

Figure 1. - View of J73-GE-1A engine in altitude chamber.

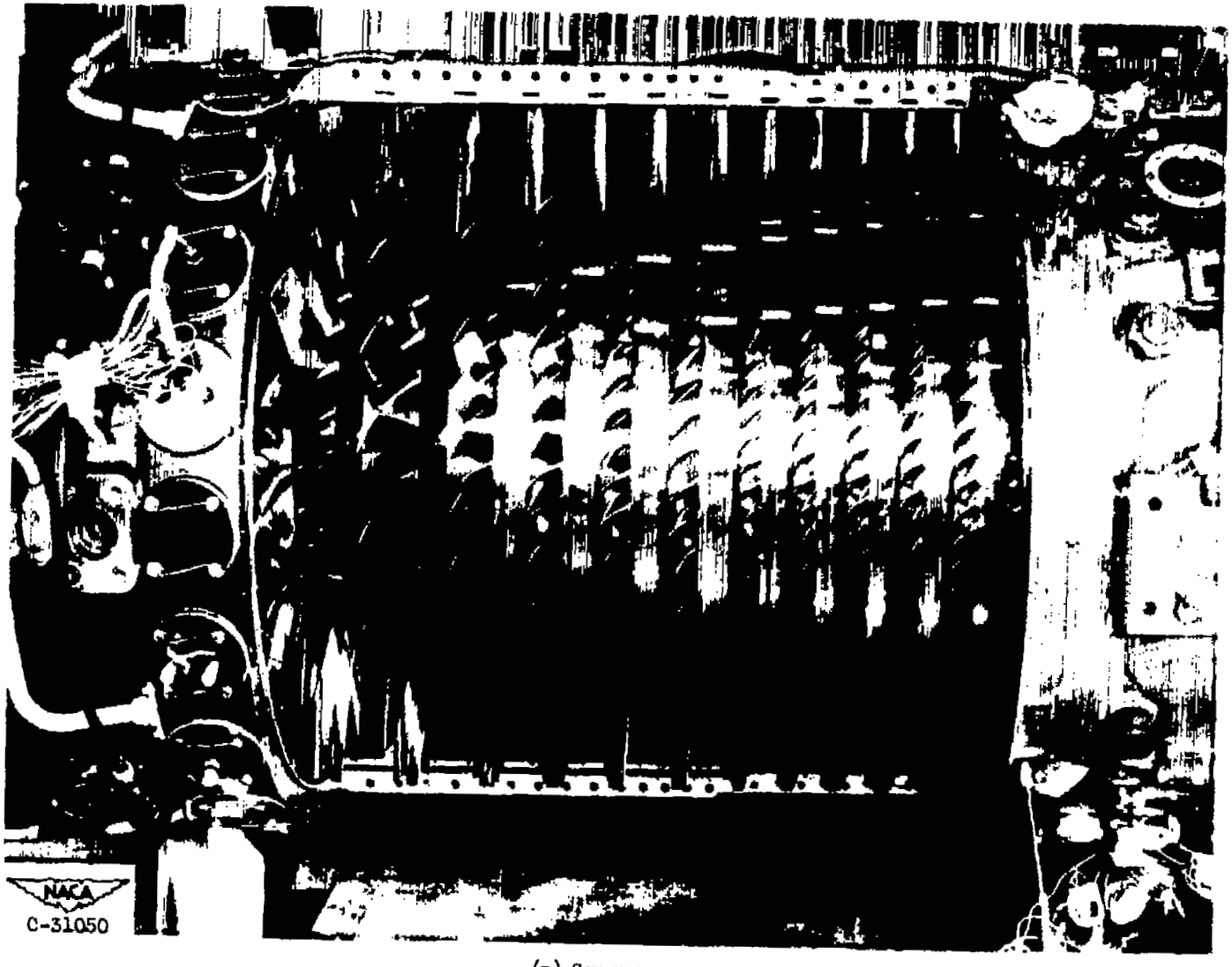

(a) Compressor.

Figure 2. - View of J73-GE-1A turbojet-engine components.

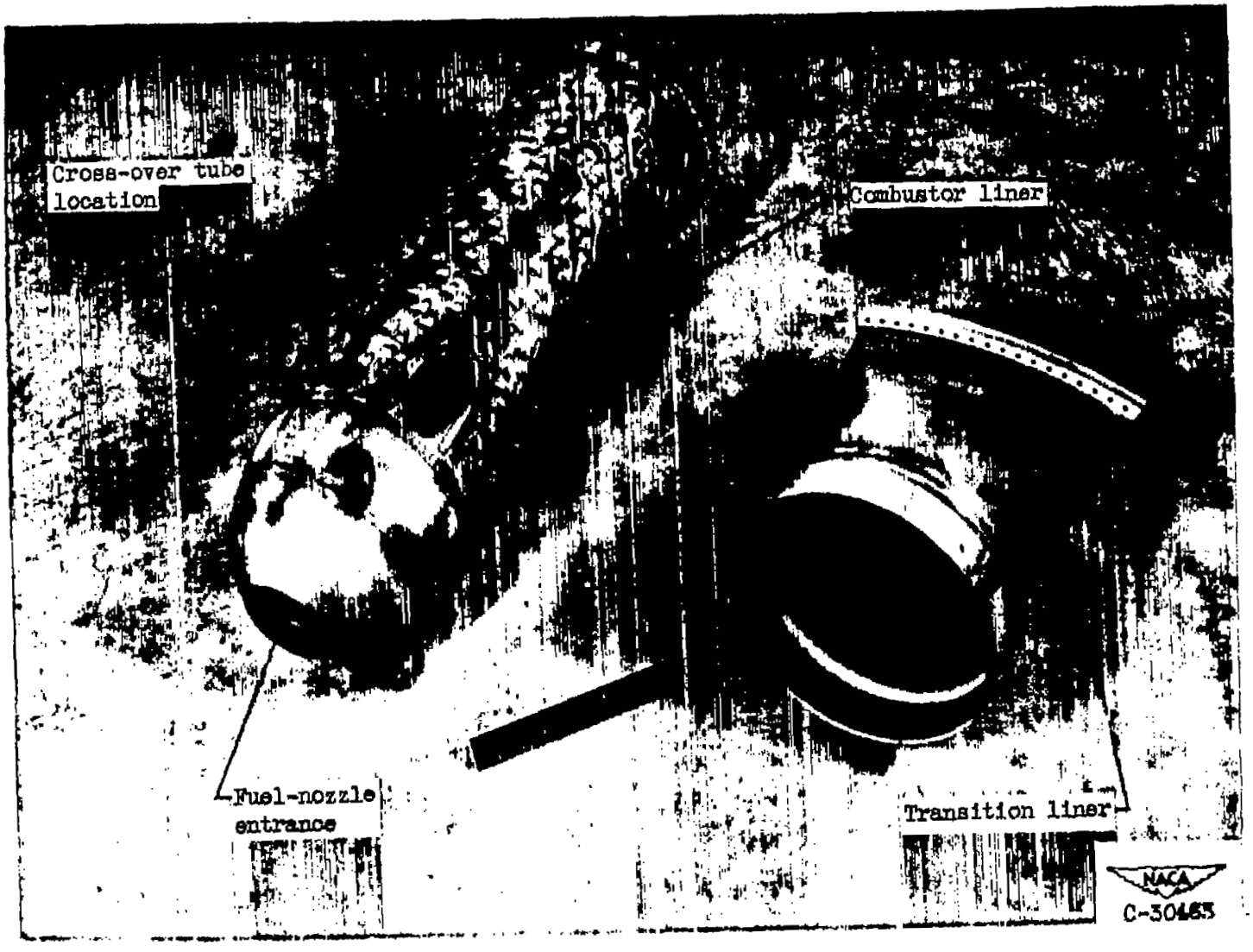

(b) Combustor and transition liners.

Figure 2. - Continued. View of J73-GE-1A turbojet-engine components.

(c) First- and second-stage turbine wheel assemblies.

Figure 2. - Concluded. View of J73-GE-1A turbojet-engine components.

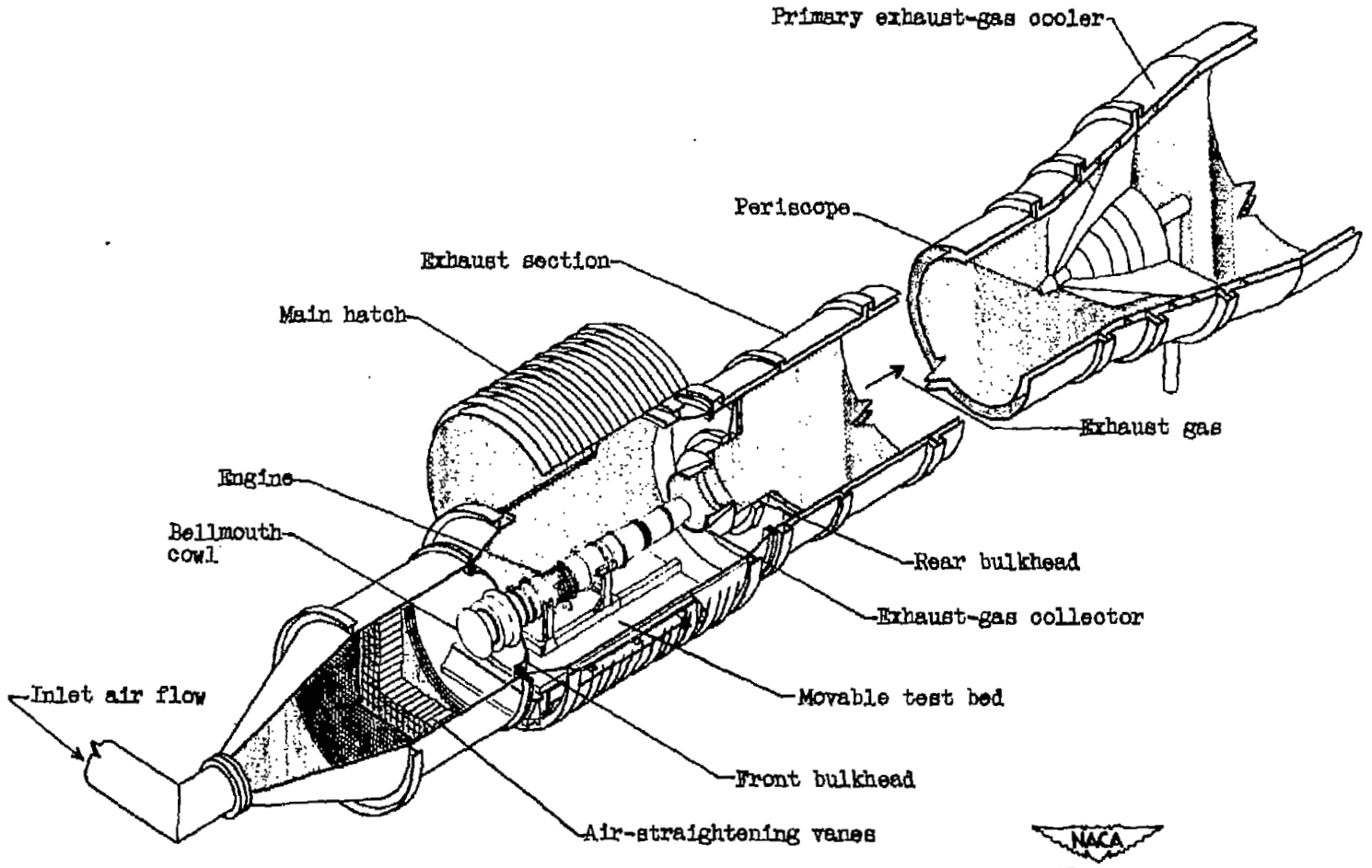

Figure 3. - Altitude chamber with engine installed in test section.

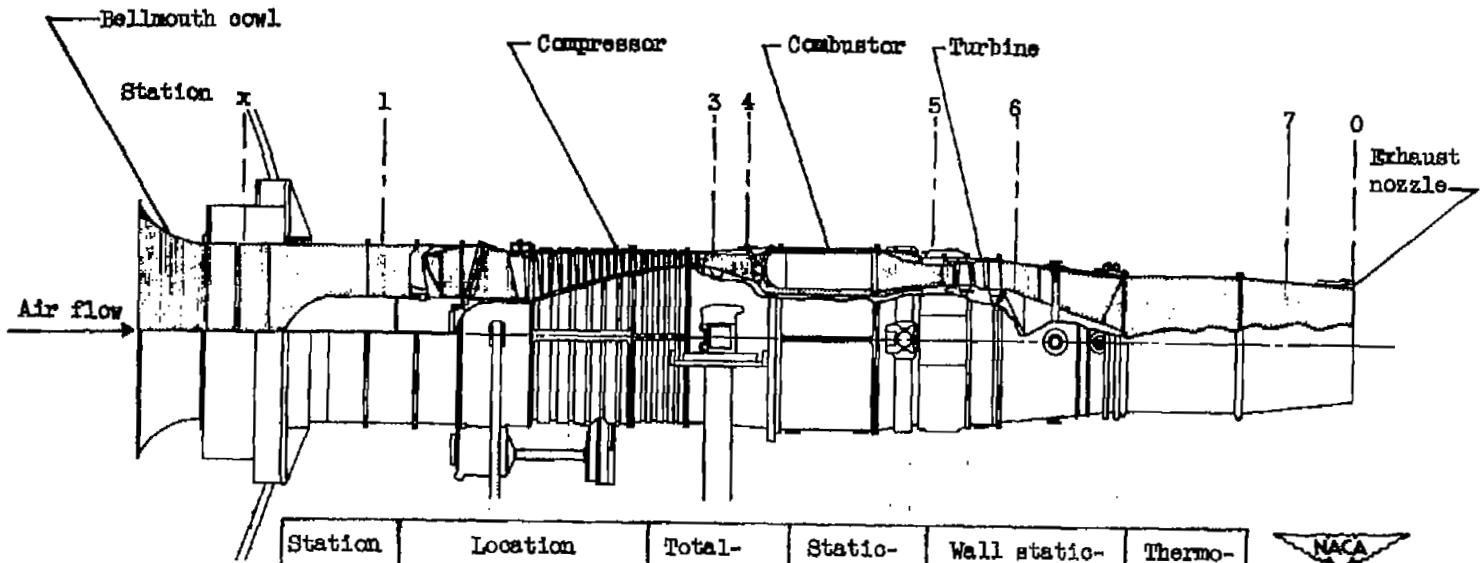

Station	Location	Total-pressure tubes	Static-pressure tubes	Wall static-pressure orifices	Thermo-couples
1	Engine inlet	36	16	4	16
3	Compressor outlet	20	4	5	6
4	Combustor inlet	5	0	0	0
5	Turbine inlet	9	0	0	0
6	Turbine outlet	24	0	8	20
7	Exhaust-nozzle inlet	28	16	4	20

NACA
CD-3088

Figure 4. - Cross section of turbojet engine showing stations at which instrumentation was installed.

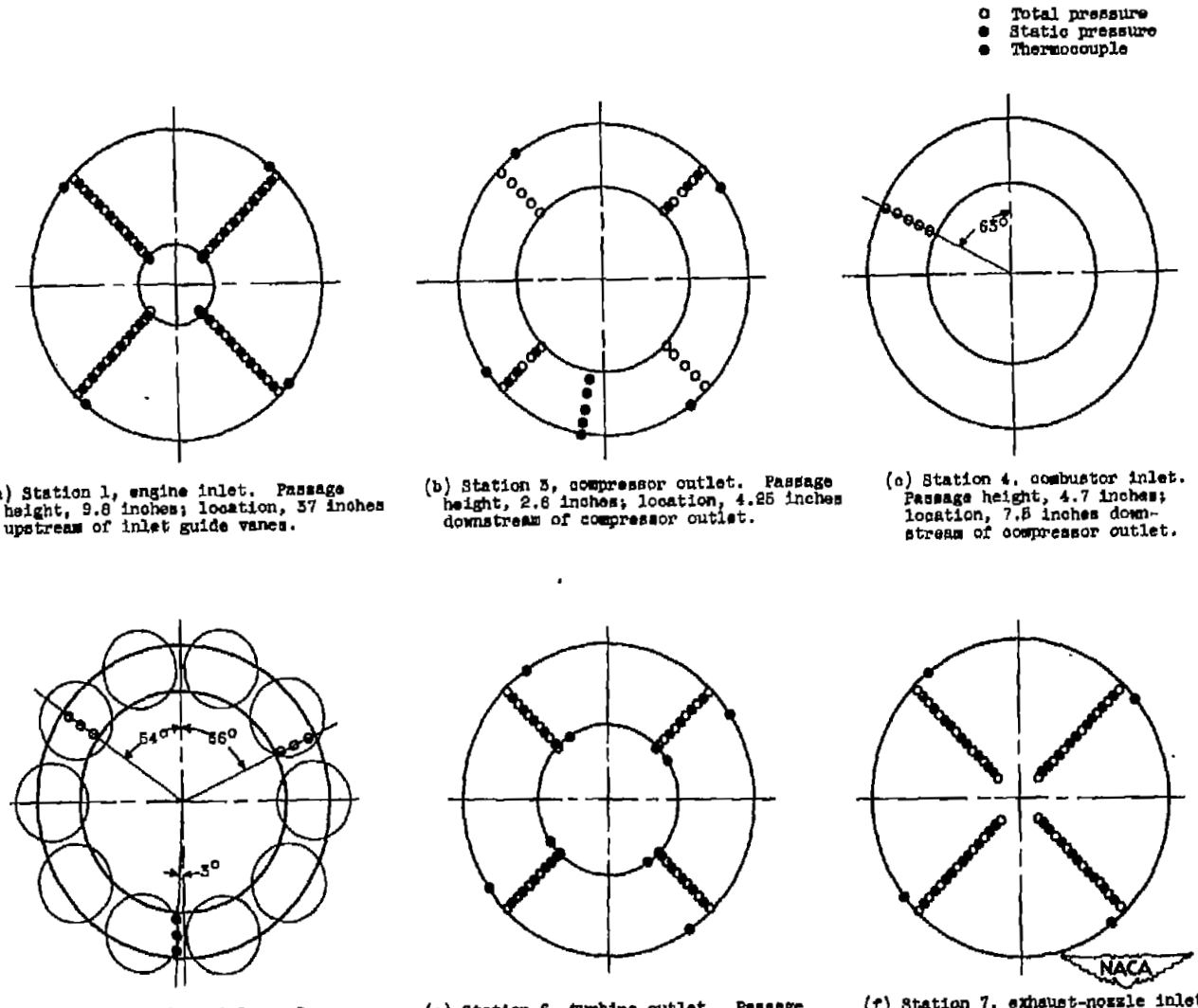

(a) Station 1, engine inlet. Passage height, 9.8 inches; location, 37 inches upstream of inlet guide vanes.

(b) Station 3, compressor outlet. Passage height, 2.6 inches; location, 4.25 inches downstream of compressor outlet.

(c) Station 4, combustor inlet. Passage height, 4.7 inches; location, 7.8 inches downstream of compressor outlet.

(d) Station 5, turbine inlet. Passage height, 4.5 inches; location, 2.3 inches upstream of turbine-nozzle leading edge.

(e) Station 6, turbine outlet. Passage height, 6 inches; location, 3.2 inches downstream of turbine outlet.

(f) Station 7, exhaust-nozzle inlet. Diameter, 23.5 inches; location, 11.8 inches upstream of exhaust-nozzle outlet.

Figure 5. - Location of instrumentation (view looking downstream).

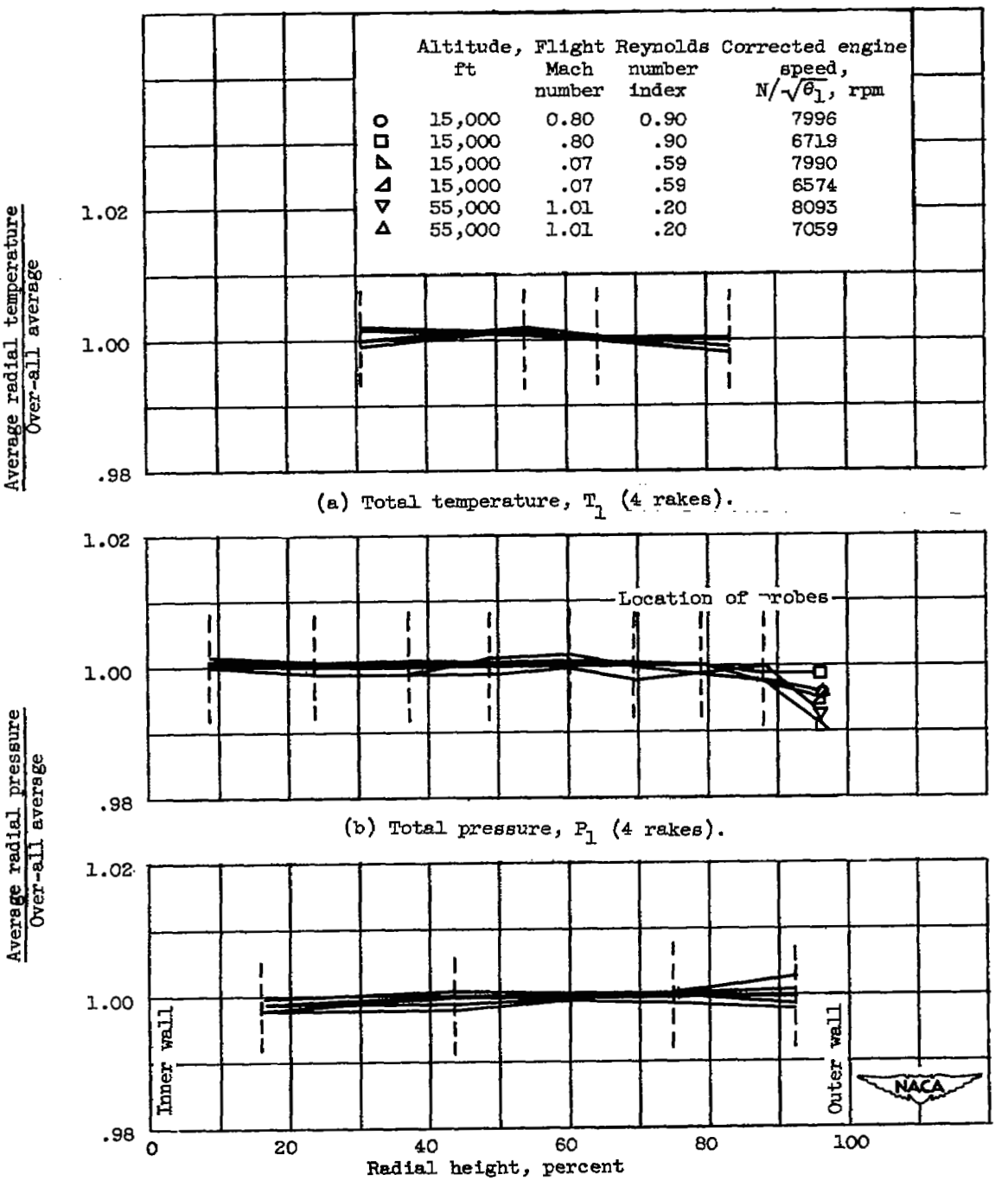

(a) Total temperature, T_1 (4 rakes).

(b) Total pressure, P_1 (4 rakes).

(c) Static pressure, p_1 (4 rakes).

Figure 6. - Pressure and temperature profiles at engine inlet, station 1.

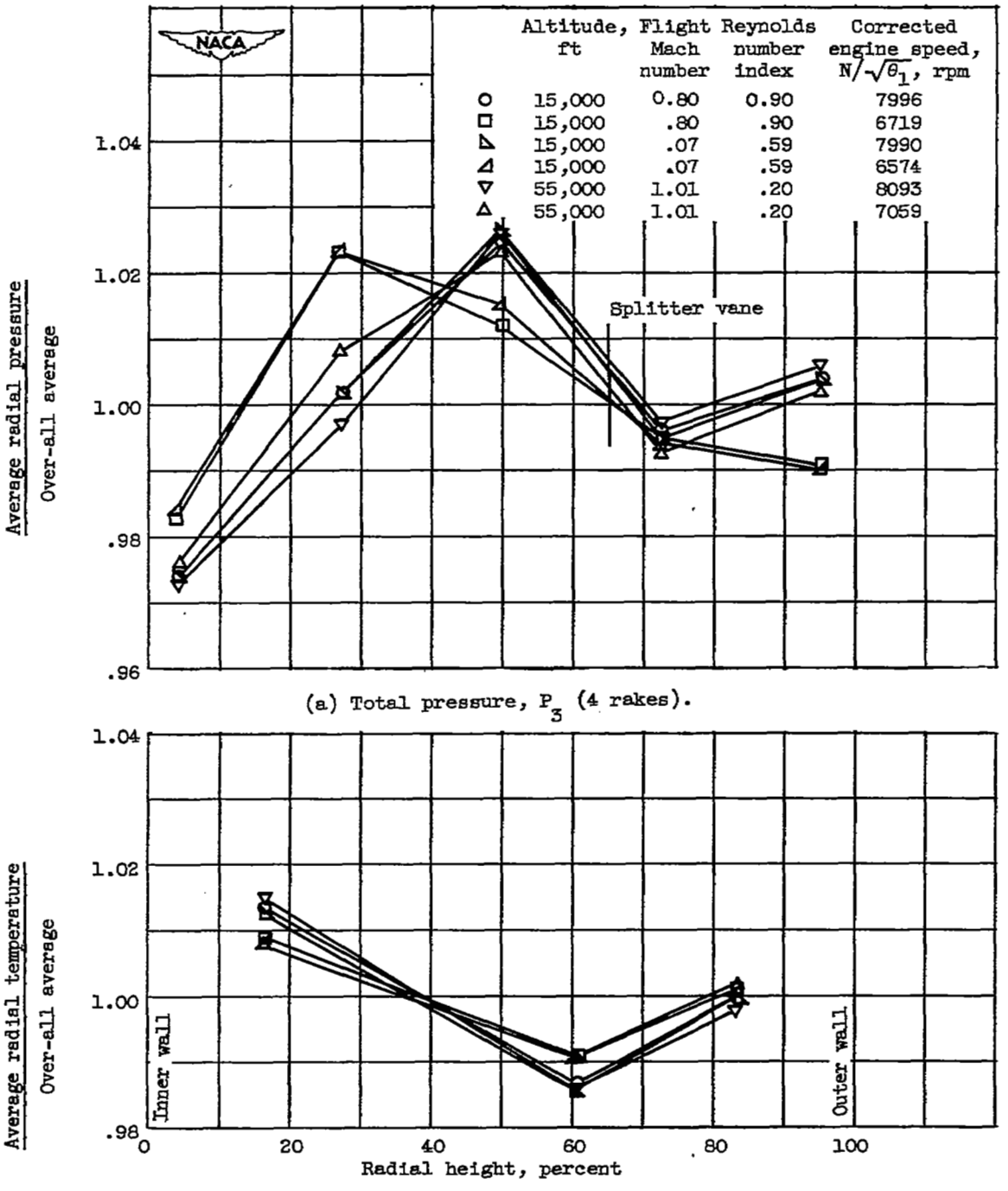

(a) Total pressure, P_3 (4 rakes).

(b) Total temperature, T_3 (2 rakes).

Figure 7. - Pressure and temperature profiles at compressor outlet, station 3.

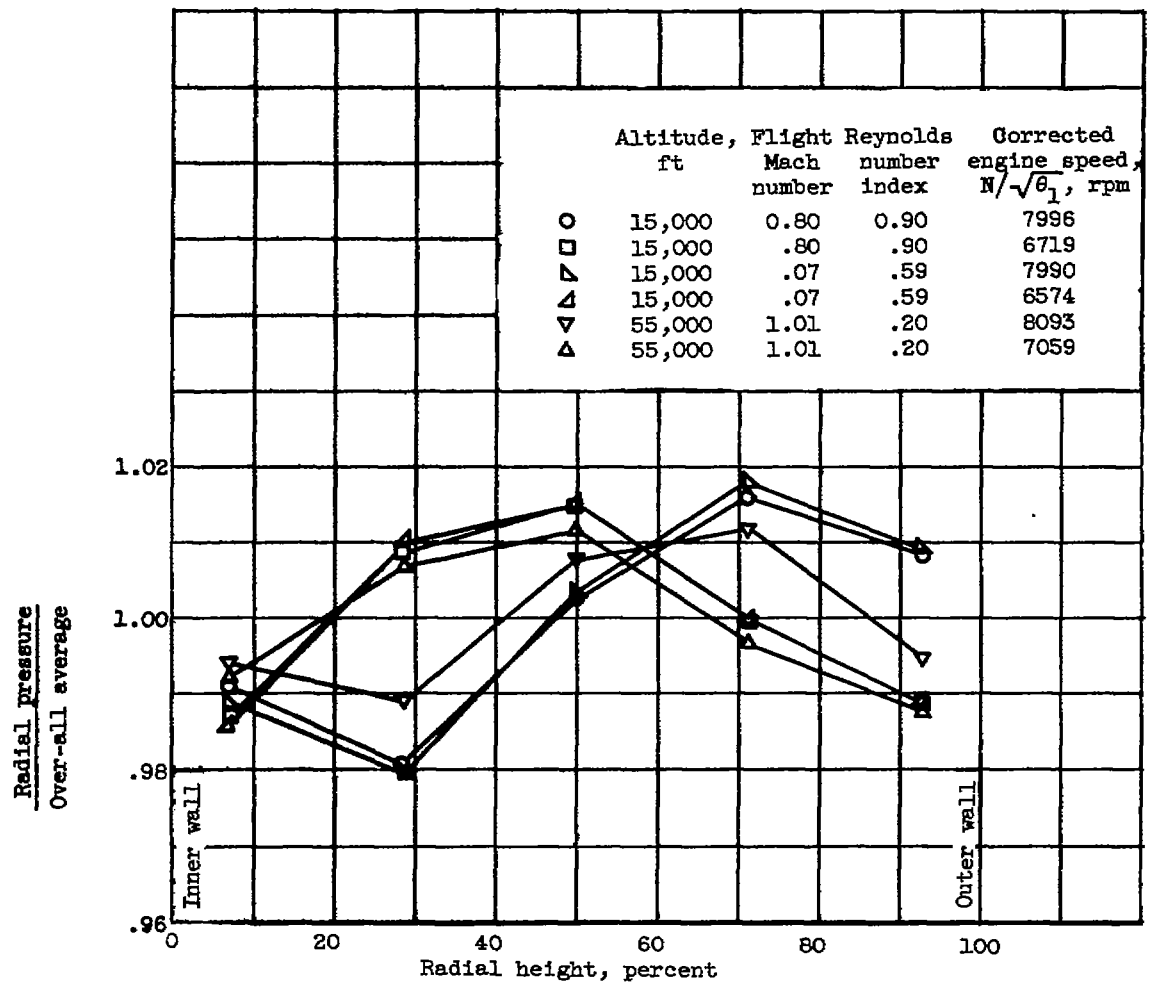

Figure 8. - Total-pressure profiles at outlet of compressor-outlet diffuser, station 4 (1 rake).

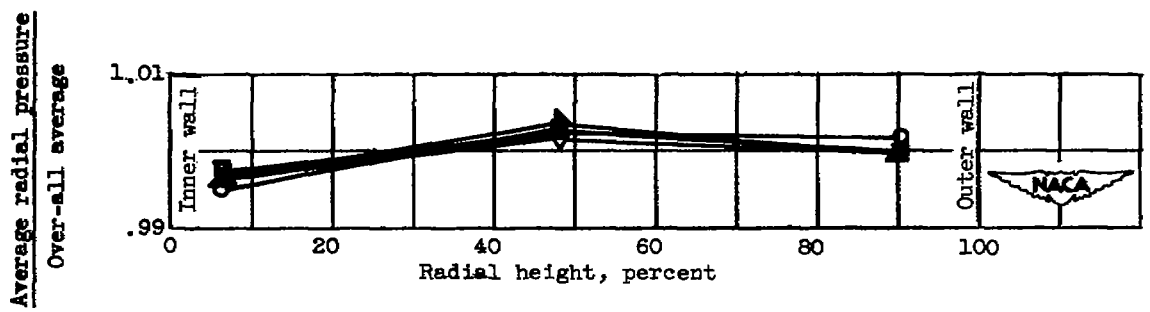

Figure 9. - Total-pressure profiles at turbine inlet, station 5 (3 rakes).

[redacted]

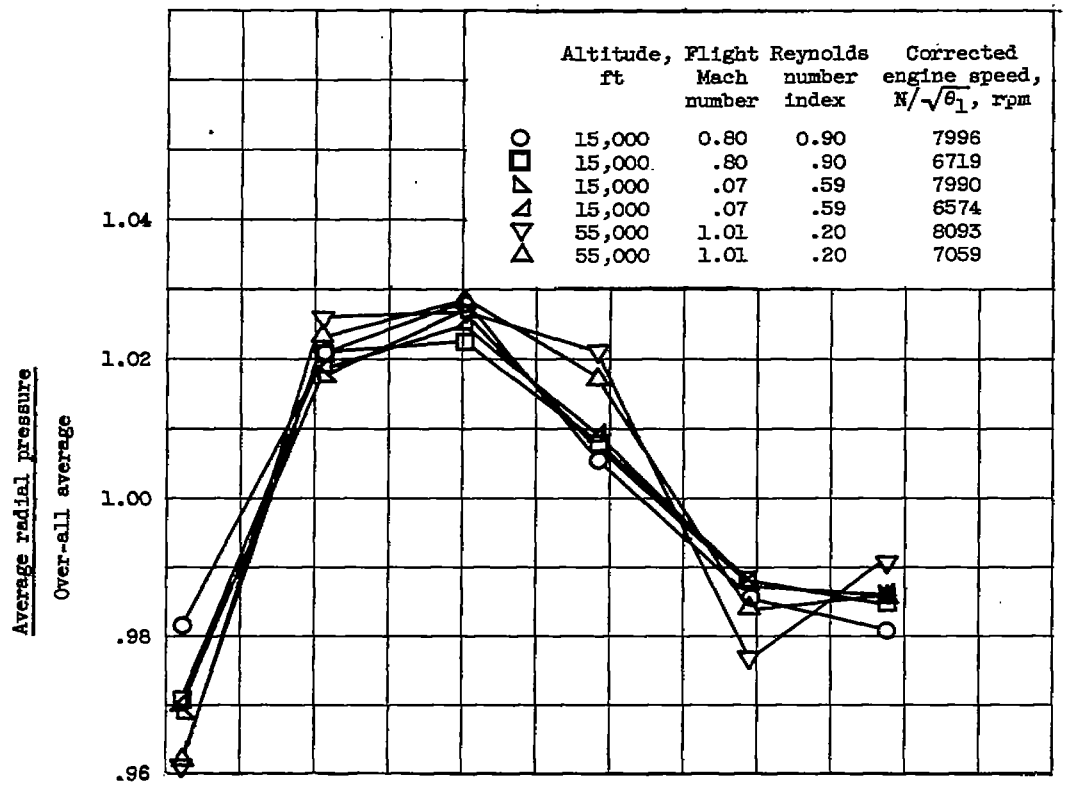

(a) Total pressure, P_6 (4 rakes).

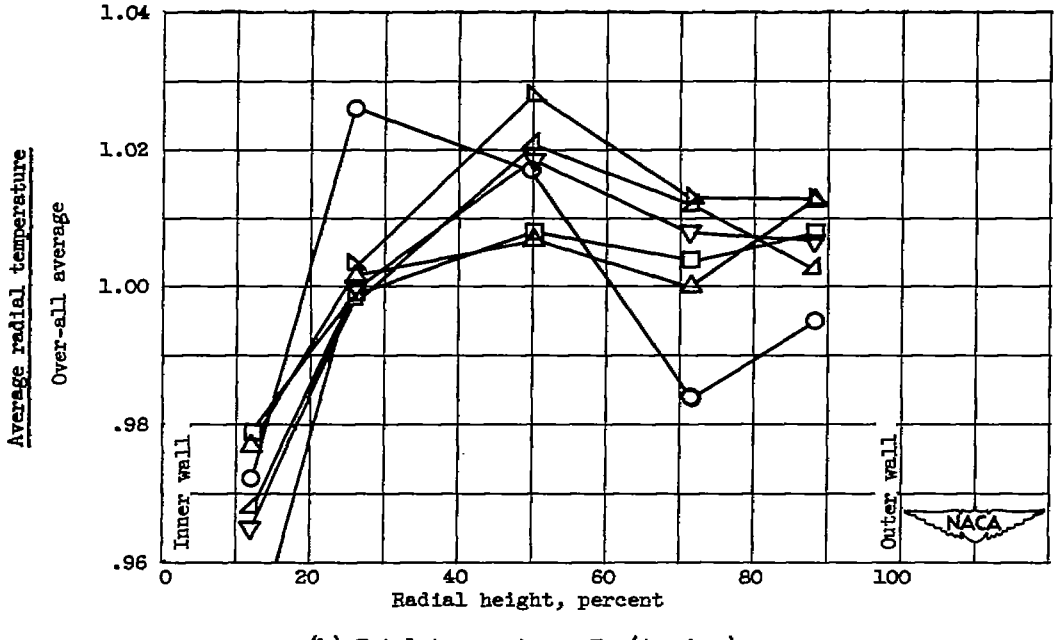

(b) Total temperature, T_6 (4 rakes).

Figure 10. - Pressure and temperature profiles at turbine outlet, station 6.

[redacted]

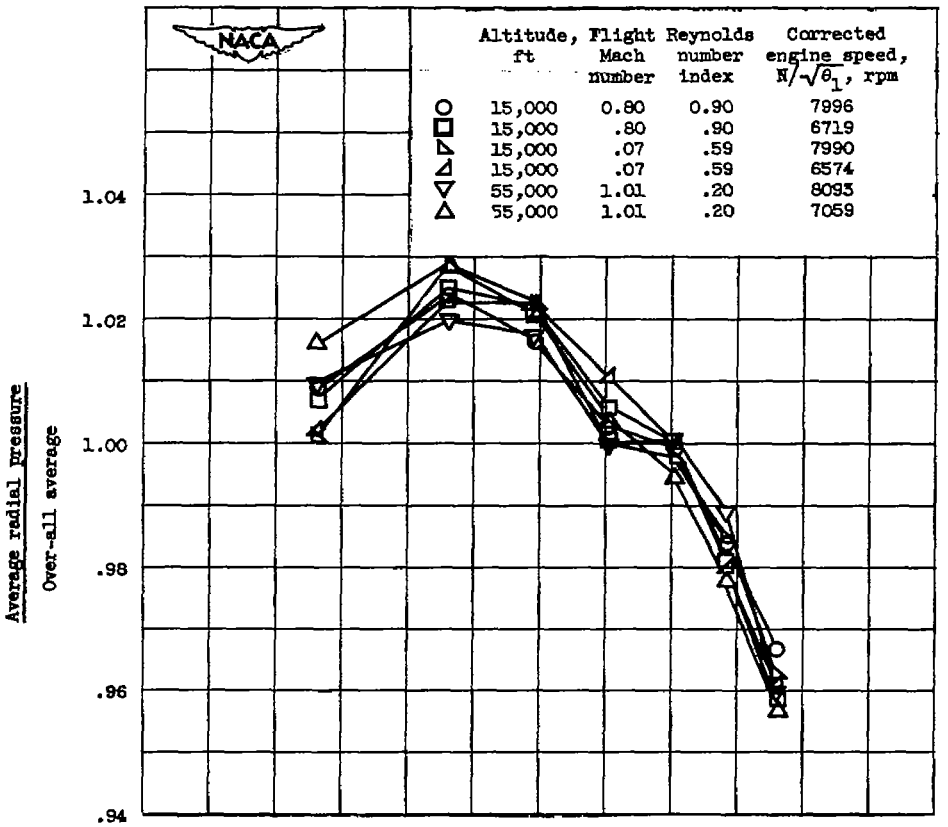

(a) Total pressure, P_7 (4 rakes).

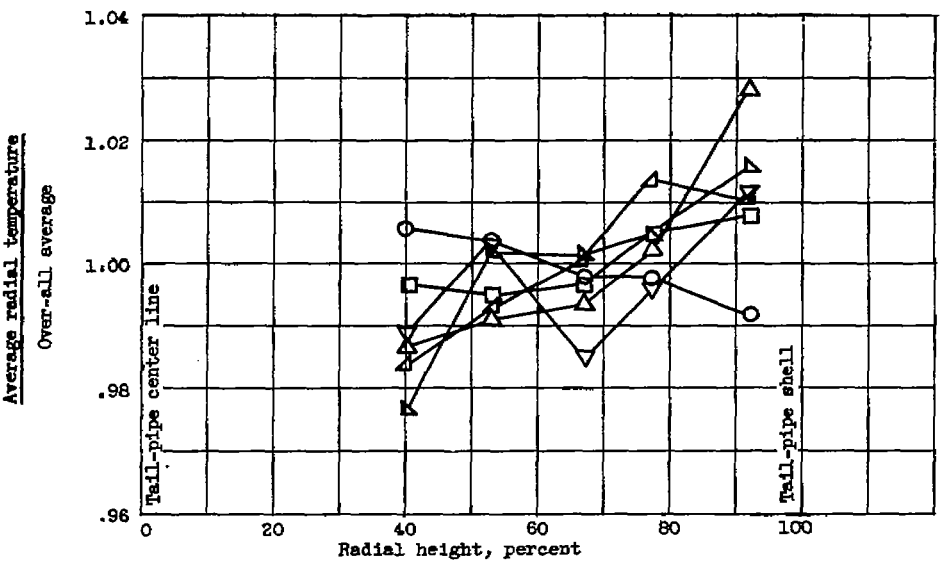

(b) Total temperature, T_7 (4 rakes).

Figure 11. - Pressure and temperature profiles at exhaust-nozzle inlet, station 7.

[redacted]

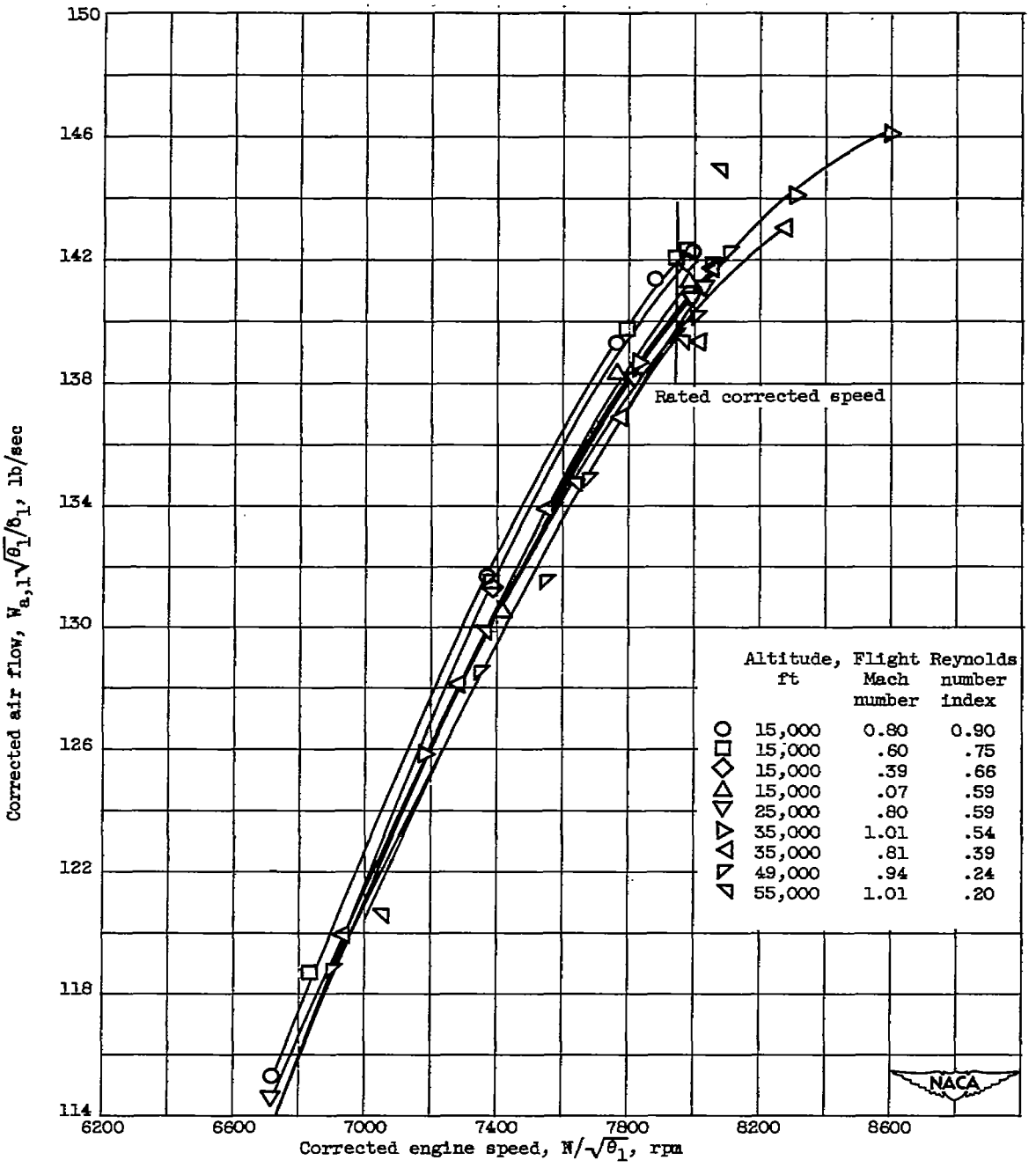

(a) Corrected air flow.

Figure 12. - Compressor performance.

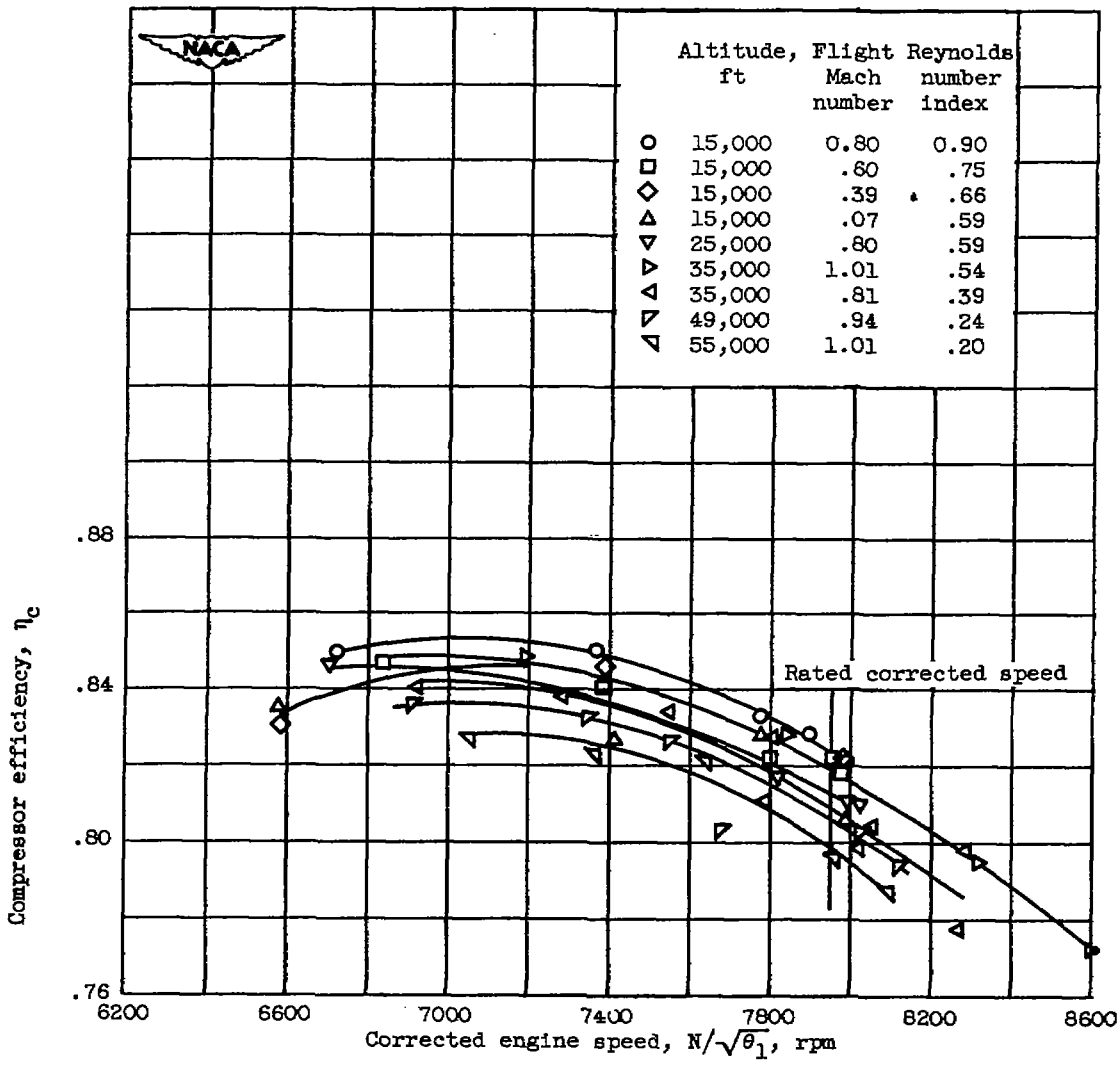

(b) Compressor efficiency.

Figure 12. - Continued. Compressor performance.

[redacted]

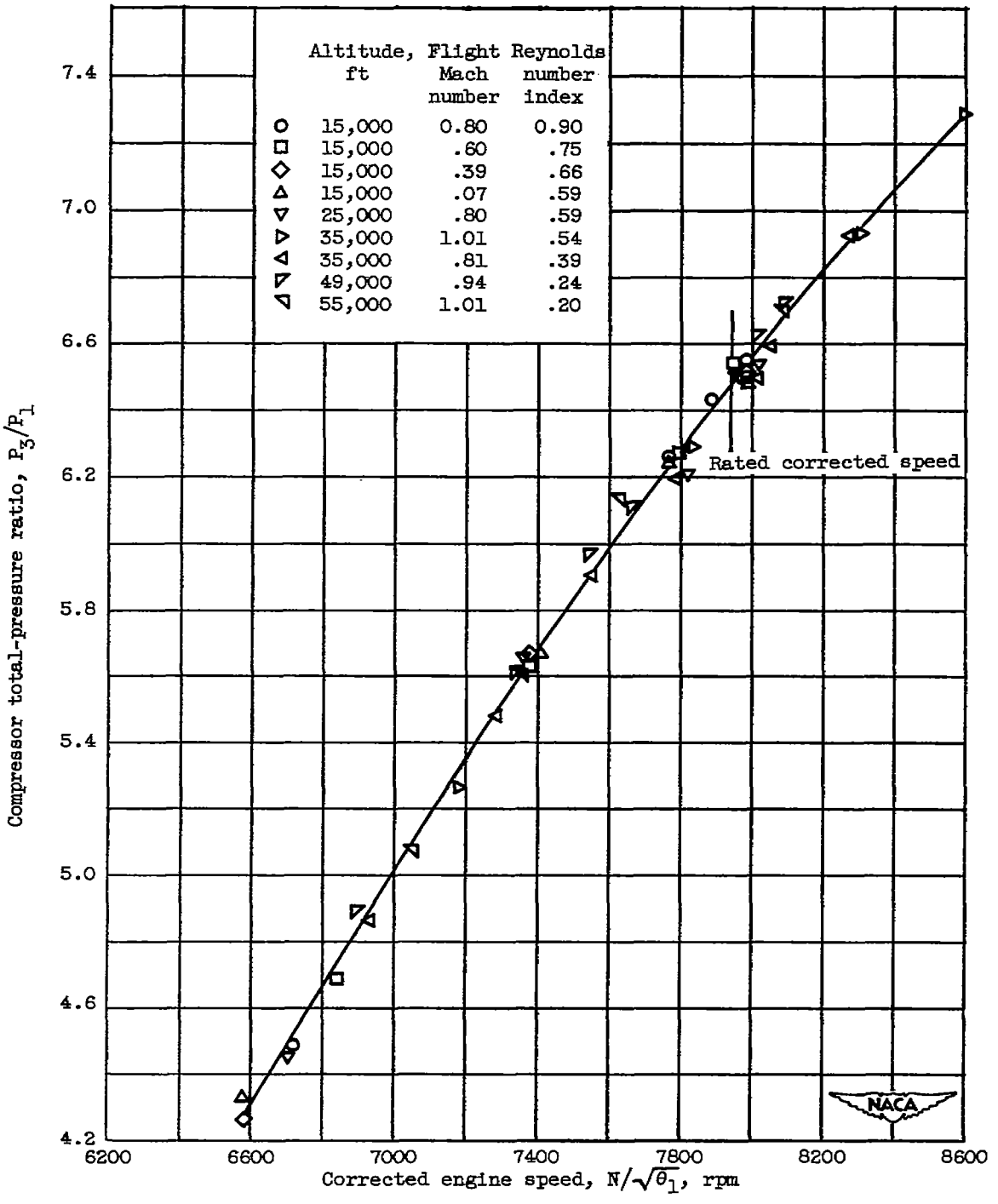

(c) Compressor total-pressure ratio.

Figure 12. - Concluded. Compressor performance.

[redacted]

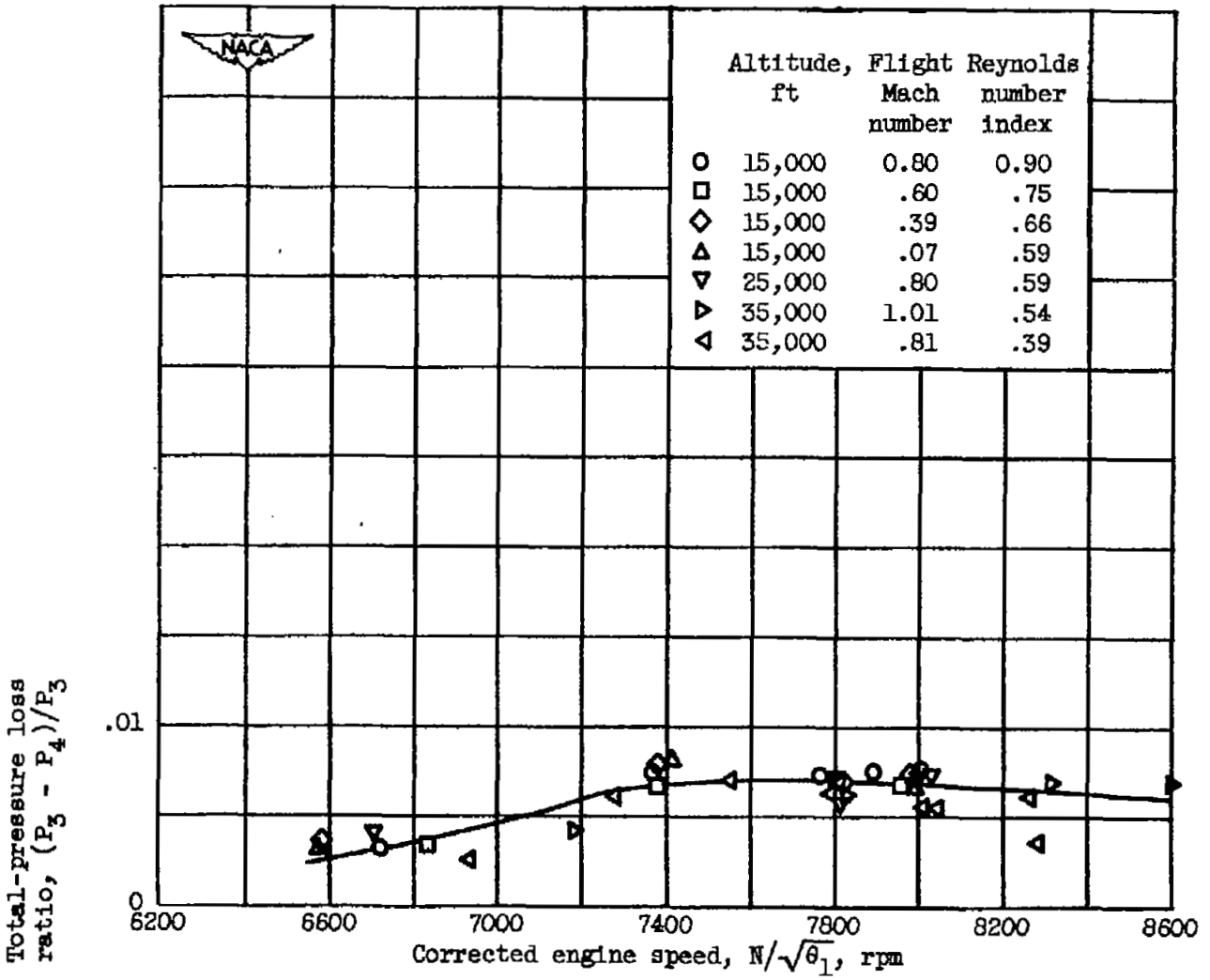

Figure 13. - Compressor-outlet-diffuser total-pressure loss.

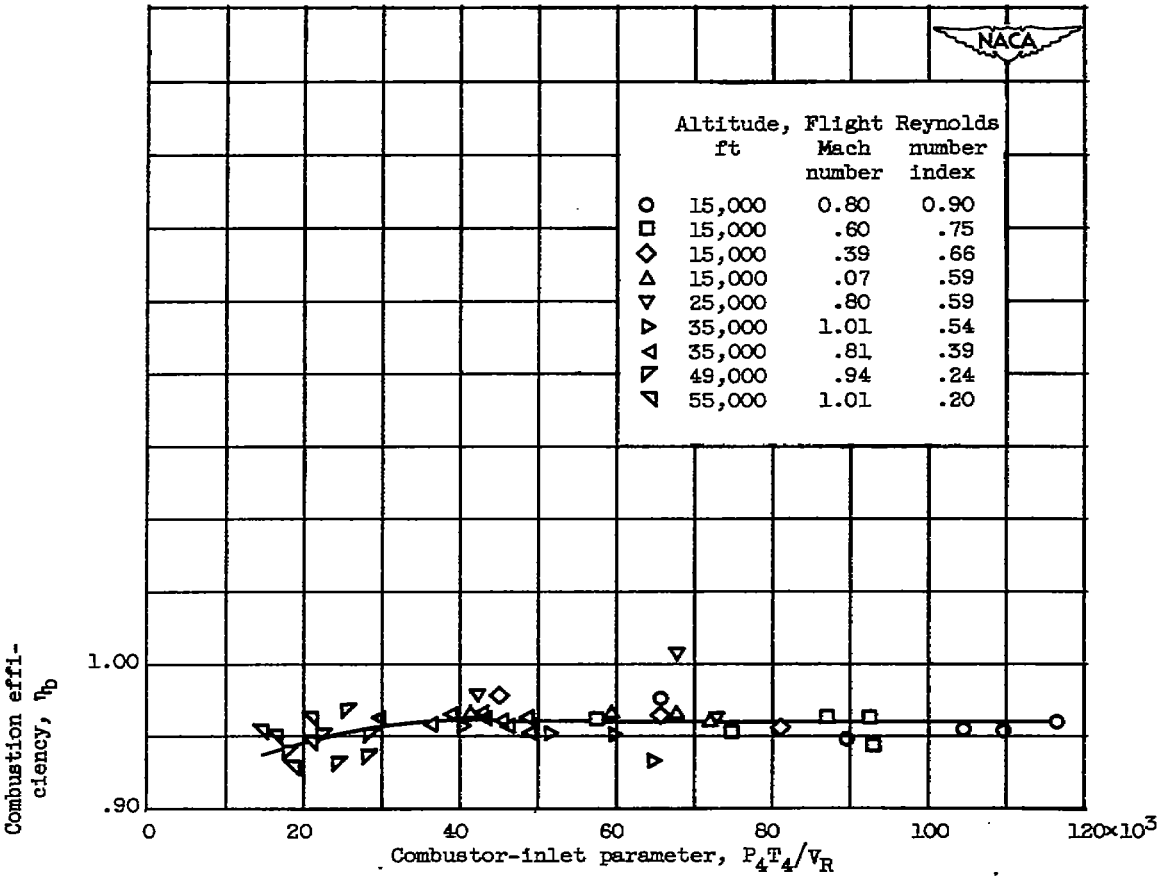

(a) Combustion efficiency.

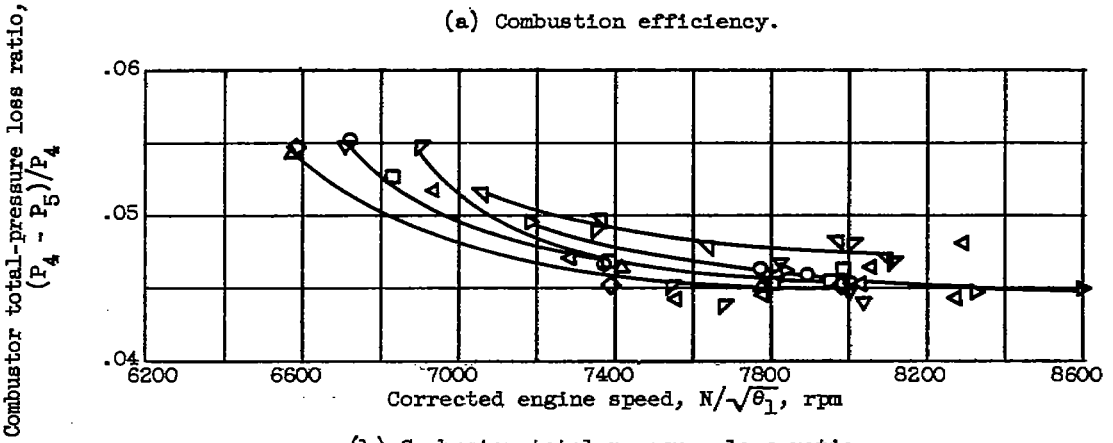

(b) Combustor total-pressure loss ratio.

Figure 14. - Combustor performance.

[redacted]

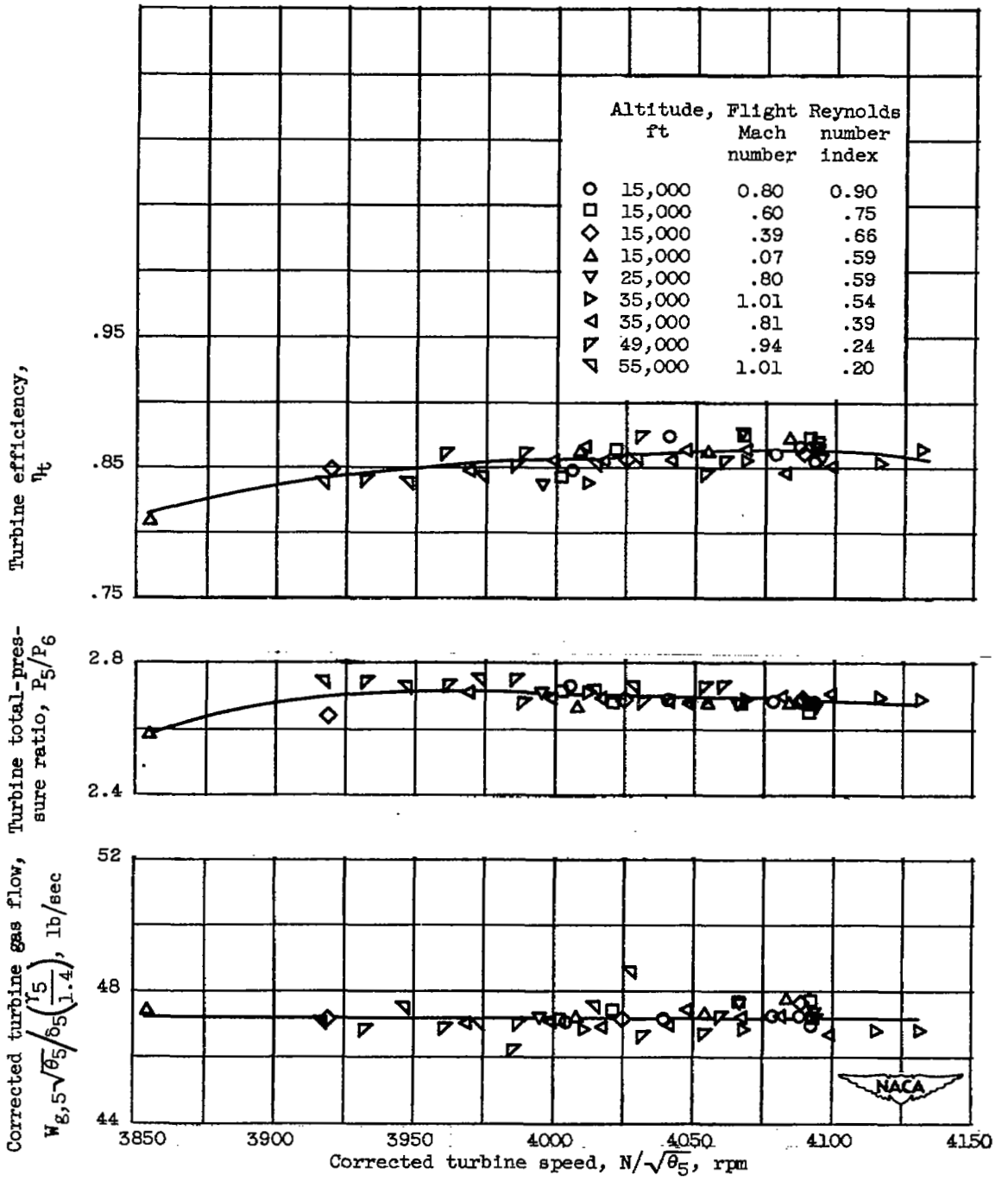

Figure 15. - Turbine performance.

[redacted]

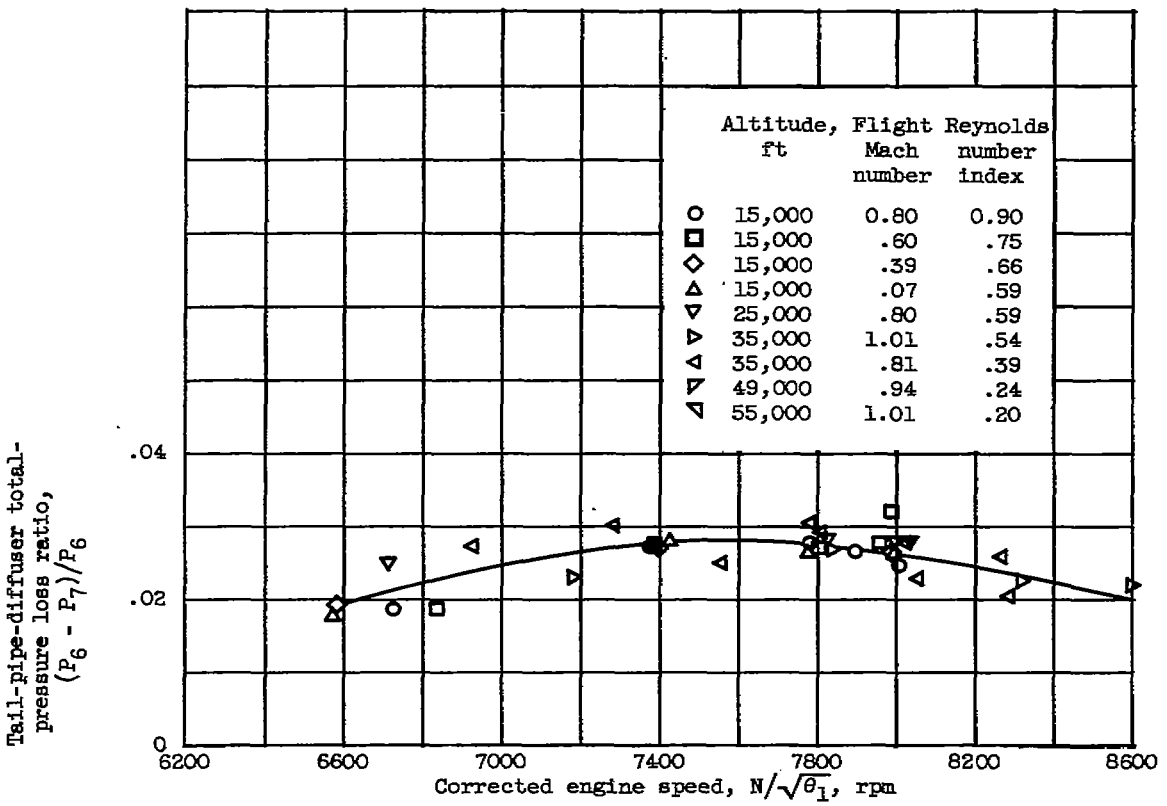

Figure 16. - Tail-pipe-diffuser total-pressure loss.

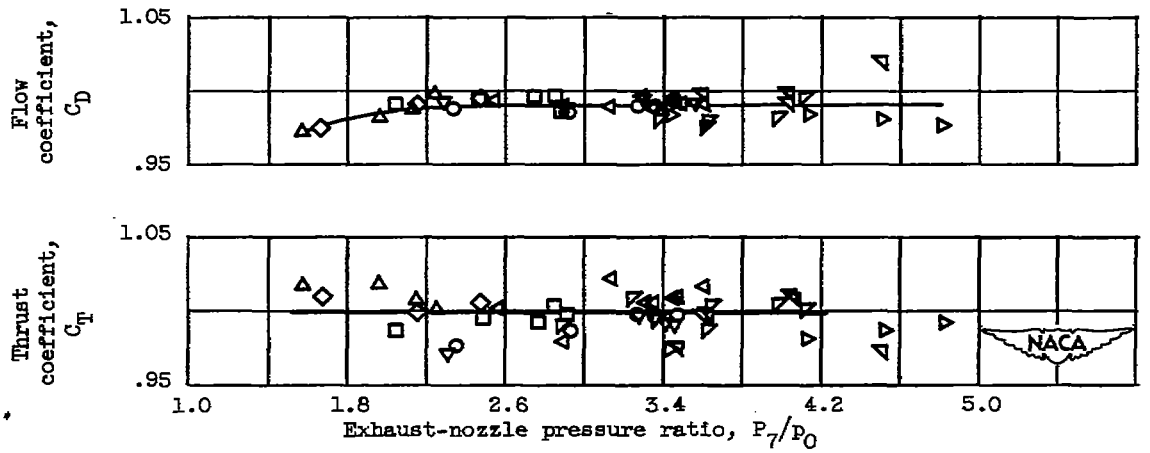

Figure 17. - Exhaust-nozzle performance.

NACA-Langley - 12-9-54 - 350